Nano Research

Open Access

Review Article

Bio-inspired locomotion of functional materials-based small-scale soft robots

Ruitong Yang[1,§], Qijian Liu[1,§], Xinlin Qing[1], Yanting Liu[2] ✉, and Yuanyuan Yang[1] ✉

[1] School of Aerospace Engineering, Xiamen University, Xiamen 361000, China
[2] Department of Applied Physics, The Hong Kong Polytechnic University, Hong Kong, China
[§] Ruitong Yang and Qijian Liu contributed equally to this work.

Cite this article: *Nano Research*, **2026**, *19*, 94908684. https://doi.org/10.26599/NR.2026.94908684

ABSTRACT: Soft robotics, as an interdisciplinary field, has attracted significant attention due to its diverse applications. With the advancement of functional materials, various soft actuators have been developed to construct small-scale soft robots. Inspired by creatures in nature, these robots exhibit unique locomotion mechanisms by regulating their actuators. In this work, we summarize the functional materials utilized in small-scale soft robots and the corresponding locomotion methods, emphasizing the working principles and actuation effects of different materials. Additionally, the characteristics of various biomimetic locomotion strategies are analyzed and discussed. This review provides valuable insights into the diverse locomotion strategies of small-scale soft robots, offering a comprehensive understanding to drive future innovations in intelligent robotic systems.

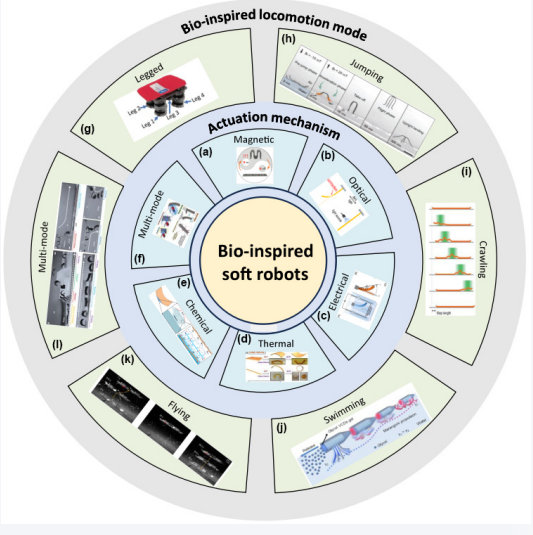

KEYWORDS: biomimetic robots, functional material, soft robotics, bio-inspired locomotion, soft actuators

1 Introduction

Soft robotics is an interdisciplinary field that combines robotics and materials science, drawing increasing attention for its flexibility and adaptability in diverse applications such as industrial automation, environmental monitoring, and healthcare [1–3]. These qualities make them well-suited for tasks requiring gentle interactions and complex motions. Recent research has increasingly focused on developing small-scale soft robots that can navigate highly confined spaces inaccessible to conventional rigid robots. This miniaturization not only expands the operational capabilities of soft robotics but also overcomes the spatial constraints inherent to traditional robotic systems.

Received: December 25, 2025; **Revised:** March 26, 2026
Accepted: March 30, 2026

✉Address correspondence to Yuanyuan Yang, yangyuanyuan@xmu.edu.cn; Yanting Liu, yanting.liu@polyu.edu.hk

The movement principles of small-scale soft robots are fundamentally influenced by their material properties. Elasticity enables energy storage/release for dynamic motions, compliance minimizes damage during environmental interactions, and deformability permits passive shape adaptation. These material-dictated properties create unique locomotion strategies fundamentally different from joint-based rigid systems. Notably, such mechanisms parallel biological solutions where organisms achieve remarkable mobility through controlled body deformations.

The deformable nature of soft robotic systems allows them to transcend the limitations of traditional actuation approaches. By fully exploiting material compliance and nonlinear dynamics, these systems can generate complex, whole-body motions through spatially distributed actuation. This capability enables the implementation of bio-inspired locomotion patterns that are particularly advantageous at small scales, where conventional mechanisms become impractical. The absence of rigid components facilitates smooth, continuous movements that can adapt in real-time to environmental variations and unexpected obstacles, offering superior performance in unstructured environments.

In this review, we center our discussion on the locomotion strategies of bio-inspired small-scale soft robots, highlighting the role of functional materials in facilitating diverse movement capabilities (Figs. 1(a)–1(f)) [4–9]. We then explore various structural designs and their impact on locomotion, examining specific examples of bio-inspired movements (Figs. 1(g)–1(l)) [10–15]. Finally, we discuss the current challenges in this field and outline potential directions for future research, aiming to advance the understanding and application of novel locomotion strategies in small-scale soft robotics.

2 Functional materials-based actuation mechanisms of small-scale soft robots

The locomotion of bioinspired small-scale soft robots is fundamentally enabled by actuation mechanisms employing functional materials. Unlike conventional robots that rely on rigid transmission components (e.g., gears, chains), these systems integrate smart materials directly into their actuation structures [16–18]. Through controlled exposure to external stimuli—including magnetic fields, electric fields, light, thermal gradients, and chemical energy—these materials generate precisely tuned internal stresses that produce controlled deformations and movements (Table 1). This stimulus-responsive paradigm allows soft actuators to achieve complex motions without traditional mechanical assemblies.

2.1 Magnetic-responsive materials for actuation

Magnetic-responsive soft actuators can achieve specific functions in environments with an external magnetic field, showing great potential in areas such as minimally invasive surgery and complex terrain observation [19–23]. These actuators primarily utilize three types of materials: magnetic elastomers, magnetic liquids, and magnetic multi-phase composites, each offering distinct actuation mechanisms.

2.1.1 Magnetic-responsive elastomer materials

The magnetic materials could exhibit macroscopic deformation under the magnetic field by embedding magnetic particles within elastomers. When an external magnetic field is applied, the magnetic inclusions experience forces or torques as a cohesive unit, thereby inducing overall, macroscopic deformation of the material. Research by Brisbois et al. [24] indicates that the magnetoelastic parameter of magnetic elastomers determines the configuration of

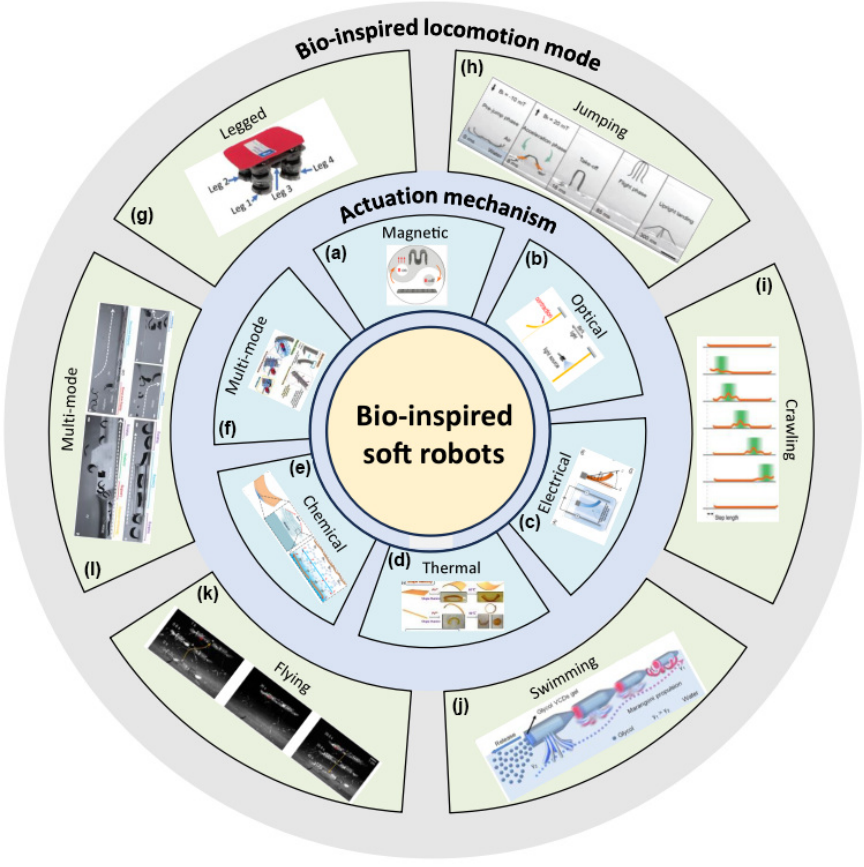

Figure 1 Overview of bioinspired soft robots. Common functional materials used for preparing bioinspired soft robots include magnetic-responsive materials (a), optical-responsive materials (b), electric-responsive materials (c), thermal-responsive materials (d), chemical-responsive materials (e), and multimodal-responsive materials (f). Reproduced with permission from Ref. [4], © American Chemical Society 2021. Reproduced with permission from Ref. [5], © American Chemical Society 2020. Reproduced with permission from Ref. [6], © American Chemical Society 2021. Reproduced with permission from Ref. [7], © Elsevier Ltd. 2024. Reproduced with permission from Ref. [8], © American Chemical Society 2024. Reproduced with permission from Ref. [9], © Wiley-VCH GmbH 2023. Common locomotion modes include legged movement (g), jumping (h), crawling (i), swimming (j), flying (k), and multi-modal locomotion patterns (l). Reproduced with permission from Ref. [10], © Atia, M. G. B. et al. 2022. Reproduced with permission from Ref. [11], © Wang, Y. B. et al. 2023. Reproduced with permission from Ref. [12], © WILEY-VCH Verlag GmbH & Co. KGaA, Weinheim 2016. Reproduced with permission from Ref. [13], © Wiley-VCH GmbH 2021. Reproduced with permission from Ref. [14], © Chen, Y. F. et al. 2019. Reproduced with permission from Ref. [15], © Macmillan Publishers Limited, part of Springer Nature 2018.

Table 1 A summary of stimuli-responsive materials

Actuation strategies	Advantages	Disadvantages	Categories	Material	Stress (MPa)	Refs.
Magnetic-responsive	Tetherless, highly penetrable, capable of multi-degree-of-freedom shape evolution, and highly biosafety	Magnetic field strength decreases rapidly with distance, the external magnetic field generating device is large and complex	Magnetic-responsive elastomer	Magnetic elastomer	0.04	[30]
			Magnetic-responsive liquid material	Liquid metal	N/A	[33]
			Magnetic-responsive multi-phase material	Biohybrid blood hydrogel fibre	0.1	[1]
Optical-responsive	Extremely high spatiotemporal resolution, enables remote, asymmetric, wireless, locally precise excitation	Limited optical penetration depth, potential thermal damage or photodegradation	Optical-responsive liquid crystal elastomer	Thiol-acrylate polymer/PDA	0.3	[39]
			Optical-responsive carbon material	PDMS/HOCNT/PET	N/A	[43]
			Optical responsive hydrogel	$Ti_3C_2T_x$/PNIPAM	0.081	[47]
Electric-responsive	High energy conversion efficiency, fast response frequency, easy to implement linear and closed-loop dynamic control	May require high voltage to drive and are prone to breakdown, some materials are limited by diffusion rates and are easily polarized	Electric-responsive dielectric elastomer actuator	SMA/Ecoflex-0030	0.09	[50]
			Electrothermal-responsive material	VBS/HEMA/Aac/AAm	0.266	[6]
			Electric-responsive ionic material	GCN/NG/PEDOT:PSS	N/A	[62]
Thermal-responsive	Large strain output (strokes); high energy density; customizable drive threshold	Low response frequency, slow cooling process, and there is a significant hysteresis effect	Thermal-responsive liquid crystal elastomer material	PNIPAM/TOCN/PAM-Fe^{3+}	0.2	[7]
			Thermal-responsive hydrogel material	GelMA–PNIPAM	0.1	[76]
Chemical-responsive	Integrates sensing and actuation, directly extract environmental energy, autonomous logic response capabilities	Limited response speed by the mass diffusion dynamics, poor environmental stability and limited repeatability of cycles	pH-responsive material	SELP hydrogel	0.0015	[78]
			Humidity-responsive material	$Ti_3C_2T_x$ PDA-MXene/ANF	300	[8]

the elastomer, and this parameter can be controlled by the magnetoelastic modulus. Thus, the driving of magnetic elastomers can be controlled by adjusting the magnetic field without changing the mechanical or chemical environment. The actuation of this kind of magnetic elastomer is primarily achieved through the manipulation of magnetic field direction or intensity for targeted deformation, including bending, stretching, twisting, and folding [25–28].

Programmable deformation in these actuators can be realized through several approaches. One method involves engineering the spatial distribution of magnetic particles. For example, Tang et al. developed an origami-inspired magnetic soft actuator capable of complex geometries. As Fig. 2(a) shows, a magnetically responsive iris was designed with concentric folding structures composed of a dodecagonal membrane and a hollow hexagon [29]. Only rectangular regions are embedded with magnetic particles that serve as contraction elements. By adjusting the magnetic field, the actuator exhibited controlled shape deformation.

Another approach utilizes pre-designed magnetization patterns. These materials are fabricated via orienting magnetic particles under an external magnetic field prior to curing, thereby creating region-specific magnetic anisotropy. Upon application of an external magnetic field, the resulting forces or torques are not transmitted uniformly across the whole material but are instead selectively and intricately localized. Such localized interactions induce complex, spatially confined deformations, which could be quantitatively tuned by precisely adjusting the external field's intensity, direction, gradient, and frequency. For example, Zhang et al. reported a magnetic-responsive soft actuator whose deformation resulted from the interaction between the external magnetic field and the embedded, programmably magnetized NdFeB particles [4]. The specific mode of deformation depended on the actuator's initial structural design, such as the origami folding pattern. As illustrated in Fig. 2(b), the actuator is capable of complex three-dimensional patterned magnetization architectures.

Combining both particle distribution control and magnetization programming enables even more sophisticated three-dimensional deformations. Wang et al. developed a multi-physics topology optimization framework for the inverse design of magneto-active metasurfaces that can undergo programmable shape morphing in three-dimensional (3D) under external magnetic fields [30]. These metasurfaces remain planar in their initial configurations and are deformed into complex 3D target shapes. The proposed framework accounts for large-deformation kinematics and optimizes both the topologies and magnetization distributions of metasurfaces in conjunction with the directions and magnitudes of the external magnetic fields. As shown in Fig. 2(c), a hybrid fabrication procedure is used to manufacture representative designs and their programmed 3D deformations were validated, demonstrating high precision and performance in complex 3D morphing.

2.1.2 *Magnetic-responsive liquid materials*

Ferrofluids and other magnetic liquid materials offer unique advantages for soft robotic applications due to their inherent fluidity and rapid response to magnetic fields [31, 32]. These materials typically consist of colloidal suspensions of magnetic nanoparticles in carrier liquids, exhibiting both liquid properties and strong magnetic responsiveness. The distinctive characteristics of magnetic liquids enable several unique capabilities in soft robotics. These actuators can undergo substantial volumetric changes through splitting and recombination processes, allowing them to navigate through narrow constrictions that would be impassable for solid actuators. For example, Fan et al. proposed a magnetically responsive soft actuator based on ferromagnetic fluid,

as shown in Fig. 3(a) [33]. This flexible actuator, as a monolith, can achieve programmable motion under the control of a magnetic field, stretching through narrow tubes and scaling in volume through splitting and polymerization. Also, they can be reassembled into a variety of functional shapes such as micro rods, micro pies, micro trains, micro kayaks, and micro rolling pins. Thus, they are equipped with multi-terrain surface adaptability to perform a variety of complex tasks.

2.1.3 *Magnetic-responsive multi-phase materials*

Magnetic multi-phase materials represent an innovative class of actuators that combine the advantages of magnetic responsiveness

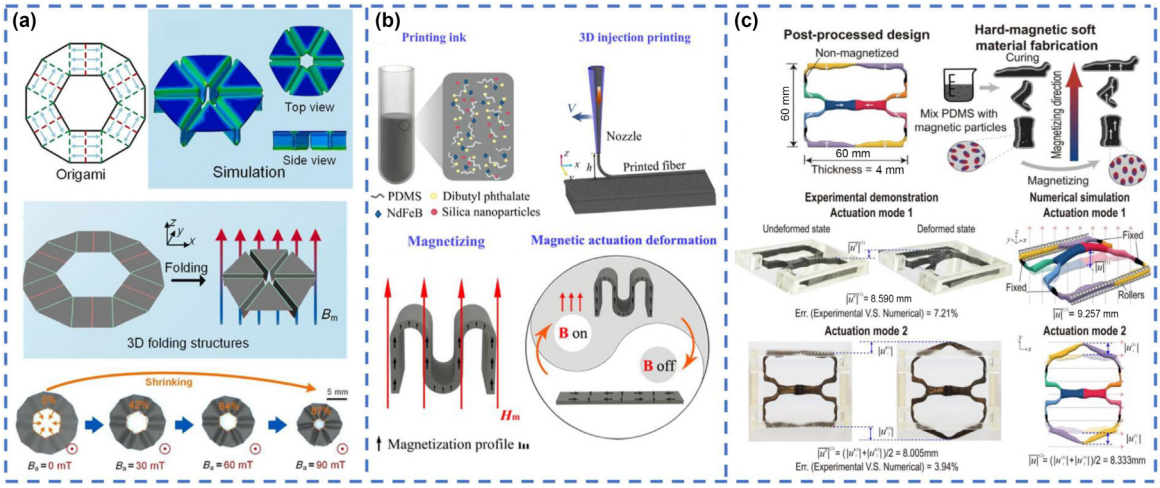

Figure 2 Magnetic-responsive elastomer materials for actuation. (a) The magnetic elastomer could implement designed macroscopic deformation by designing the distribution of magnetic particles within elastomer. Reproduced with permission from Ref. [29], © Elsevier Ltd. 2021. (b) The magnetic elastomer could implement designed macroscopic deformation by patterned pre-magnetization. Reproduced with permission from Ref. [4], © American Chemical Society 2021. (c) The magnetic elastomer could implement designed macroscopic deformation by adjusting the magnetic field. Reproduced with permission from Ref. [30], © Elsevier B.V. 2023.

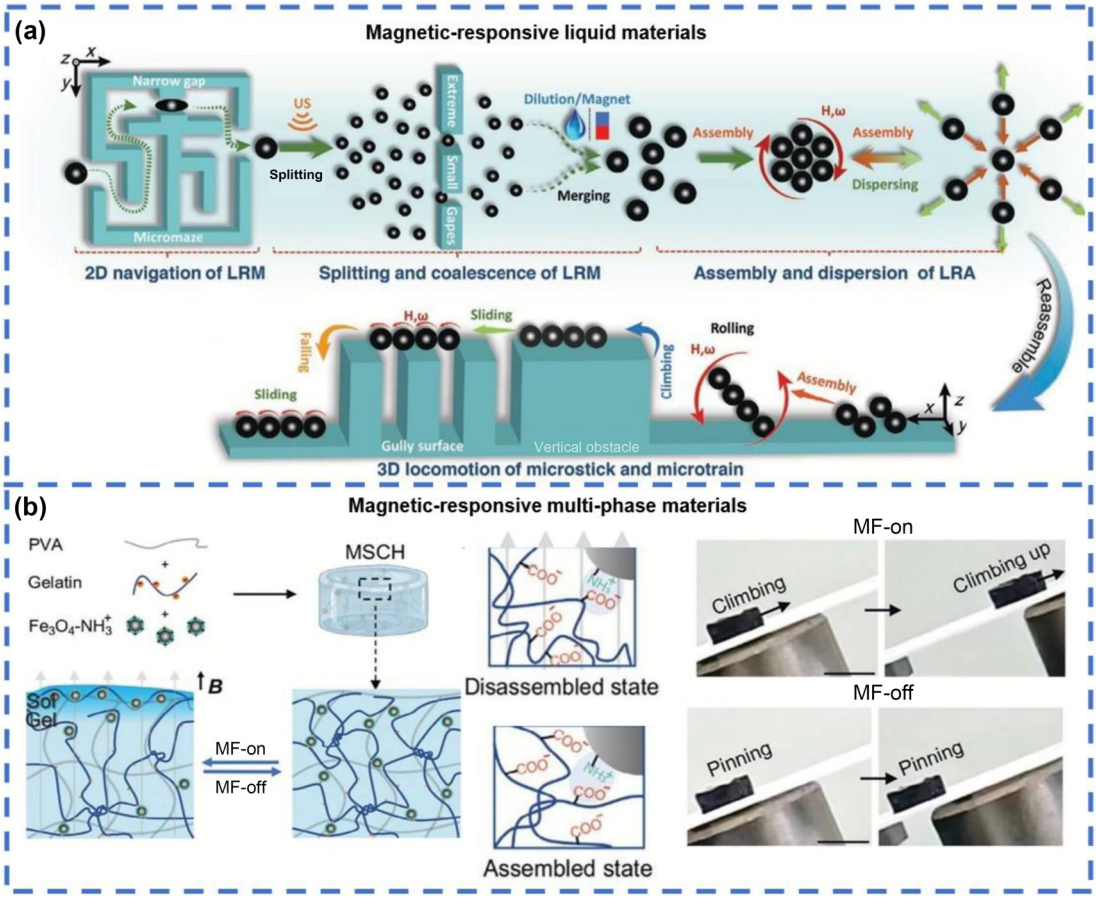

Figure 3 Magnetic-responsive liquid material for actuation. (a) Magnetic-responsive ferromagnetic fluid material. Reproduced with permission from Ref. [33], © WILEY-VCH Verlag GmbH & Co. KGaA, Weinheim 2020. (b) Magnetic-responsive multi-phase hydrogel material. Reproduced with permission from Ref. [34], © Wiley-VCH GmbH 2024.

with other functional material properties. These hybrid systems typically integrate magnetic components with stimuli-responsive polymers or hydrogels, creating materials with enhanced functionality and tunable properties. For example, Wang et al. developed a magnetic-responsive, semi-convertible hydrogel actuator based on dynamic liquid lubrication mechanisms (Fig. 3(b)) [34]. Under an external magnetic field, the actuator switched between a gel state and a gel–sol state. This transition did not involve macroscopic shape changes but was driven by forces exerted by the magnetized particles attached to the gelatin chains, triggering disassembly of the gelatin's triple-helix structures. The resulting disassembly generated a sol lubricating layer on the hydrogel surface, while the remaining network retained its structural integrity. This magnetic-field-induced gel–sol transition significantly reduced the friction coefficient, offering adjustability for magnetic actuation.

Magnetic-responsive materials enable wireless, non-contact control across media like water and biological tissues. By modulating external fields and internal magnetization profiles, these materials achieve complex 3D deformations suitable for biomedical soft robots. However, their reliance on high-energy, complex field generators and susceptibility to mutual interference in multi-body systems remain significant challenges.

2.2 Optical-responsive materials for actuation

Optical-responsive soft actuators enable targeted functionality in environments with external light sources by undergoing reversible structural deformations such as bending, contraction, or expansion, thereby facilitating controlled movement [35–37]. Owing to their advantages in wireless, remote, and localized control, optical-responsive soft actuators have attracted significant attention in recent years. By adjusting the wavelength and intensity of the applied optical field, programmed movements could be implemented [38–40]. Optical-responsive soft materials for actuation mainly include liquid crystal elastomers (LCEs), carbon-based optical-responsive materials, and optical-responsive hydrogels.

2.2.1 *Optical-responsive liquid crystal elastomer materials*

Liquid crystal elastomers, as a class of optical-responsive soft materials, combine the anisotropic properties of liquid crystals with the elastic behavior of polymer networks. These materials exhibit remarkable light-induced deformations due to their molecular architecture, where the orientation of mesogenic units within the crosslinked polymer matrix determines their macroscopic response. LCEs undergo reversible shape changes upon light exposure through photoisomerization of molecules, which generates anisotropic stresses and propagates through the network to produce macroscopic deformation. The degree and direction of actuation can be precisely controlled by tuning the light parameters (e.g., wavelength and intensity) and the initial molecular alignment, enabling programmable shape-morphing behaviors such as bending, twisting, and folding.

Recent developments have further enhanced their functionality through combining with functional additives, such as photosensitizers, metallic conductors, and chromophores within the elastomeric matrix. For example, Bao et al. [41] reported a light-responsive liquid crystal polyurethane elastomer incorporating light-triggered molecular motors (LCPU-MM) (Fig. 4(a)). These overcrowded alkene-based motors were modified with trifunctional ethylene glycol spacers in both their rotor and stator regions, enabling them to serve as crosslinkers and unidirectional stirrers within the polyurethane network. Upon exposure to specific wavelengths of light, the motors underwent conformational changes or unidirectional rotation. Such nanoscale motion was then

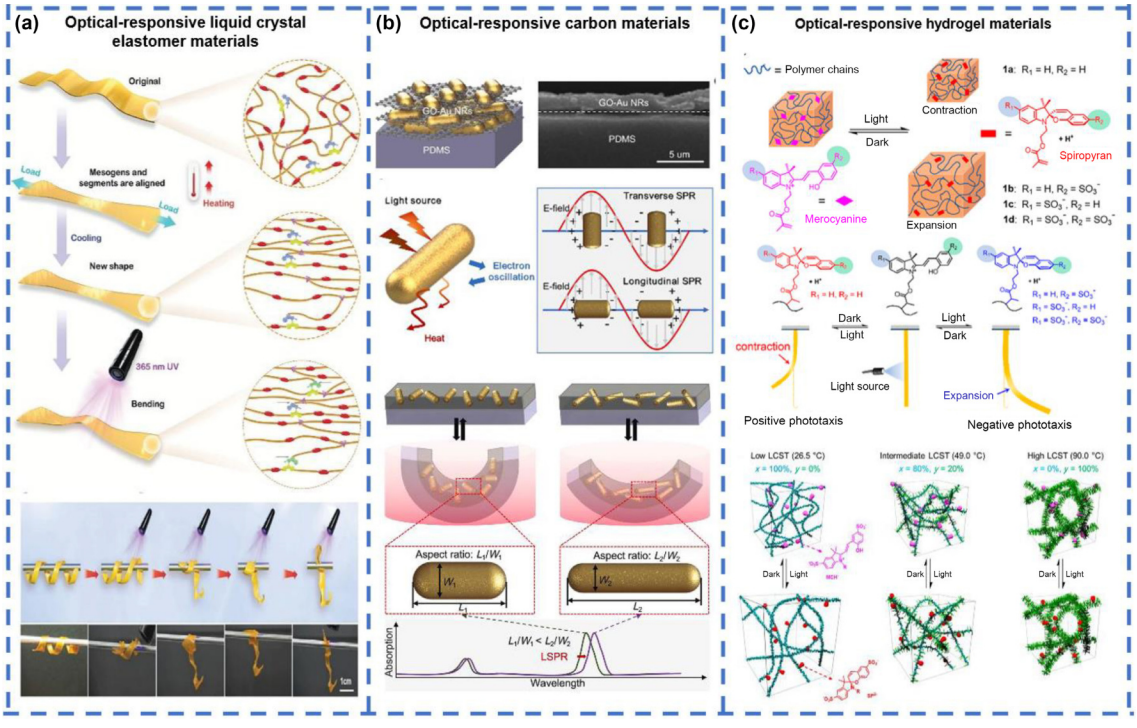

Figure 4 Optical-responsive materials for actuation. (a) Optical-responsive liquid-crystalline material. Reproduced with permission from Ref. [41], © Wiley-VCH GmbH 2023. (b) Optical-responsive carbon materials. Reproduced with permission from Ref. [45], © Li, K. C. et al. 2024. (c) Optical-responsive hydrogel material. Reproduced with permission from Ref. [5], © American Chemical Society 2020.

amplified into macroscopic deformation, endowing the actuator with large-scale, programmable shape-changing capabilities. Zhang et al. demonstrated a three-layer LCE actuator with sensing ability by integrating oriented LCE membrane with silver and carbon black layer [42]. Screen printing deposited the silver and carbon black films onto the aligned LCE, after which near-infrared irradiation of the carbon black generated heat, produced a temperature gradient across the LCE, and induced bending, further enabling the sense of the intensity, spot size, and position of NIR light.

2.2.2 *Optical-responsive carbon materials*

Carbon-based optical-responsive materials have emerged as promising candidates for soft actuators, owing to their exceptional light absorption capabilities across a broad spectrum, good photothermal conversion efficiency, and outstanding mechanical robustness. These materials, which typically include carbon nanotubes (CNTs), graphene, and carbon black dispersed in polymer matrices, operate primarily through the photothermal effect—when illuminated, the carbon nanostructures efficiently absorb photon energy and convert it into thermal energy. This localized heating induces a volume mismatch, generating internal stresses that lead to controlled macroscopic deformations such as bending, twisting, or contraction/expansion. The actuation performance can be tuned by engineering the composite's structure, including the carbon filler concentration, distribution pattern, and interfacial bonding with the polymer matrix, as well as by controlling the illumination parameters (wavelength, intensity, and spatial distribution) [43].

Currently, various optical-driven soft actuators based on carbon-based materials have been reported, showing good optical-controlled deformation ability [44]. The investigation of photothermally responsive soft actuators containing carbon materials centered on the incorporation of auxiliary fillers or novel architectures to boost photothermal conversion efficiency. Li et al. reported a light-driven soft actuator based on CNTs and the plasmonic coupling effect of gold nanorods (Au NRs) [45]. As shown in Fig. 4(b), the plasmonic effect could highly enhance the photothermal efficiency of actuator, which caused the PDMS layer to expand and the GO-Au NRs layer to shrink, resulting in interfacial stress that induced reversible bending of the actuator. Su et al. developed actuator based on a two-dimensional heterojunction of tungsten diselenide (WSe_2) and graphene nanosheets [46]. The heterostructure is embedded within a PDMS matrix via spin coating onto a passive substrate, yielding an asymmetric bilayer design. In this assembly, graphene sheets intercalated between WSe_2 layers enhanced both photothermal efficiency and thermal dissipation. The PDMS network thoroughly encapsulated the nanosheets, which conferred programmable deformation behavior under optical stimulation.

2.2.3 *Optical responsive hydrogel materials*

Photosensitive hydrogels combine the exceptional biocompatibility and soft tissue-like mechanical properties of hydrogels with light-responsive capabilities [47, 48]. The actuation mechanism operates through two primary pathways: either light-triggered alterations in the polymer network's hydrophilicity that modify water absorption capacity, or photo-induced changes in crosslinking density through cleavage or formation of chemical bonds. When activated by specific wavelengths, these molecular transformations create pressure that drives controlled swelling or deswelling of the hydrogel matrix. The combination of high-water content and biocompatibility makes photosensitive hydrogels especially valuable for biomedical applications.

Recent efforts concentrate on formulating composite hydrogels that combine components with exceptionally high photothermal conversion. Zheng et al. ultilized a composite hydrogel of poly(N-isopropylacrylamide) (PNIPAM) and Fe_3O_4 nanoparticles as the actuator medium and employed two photon polymerization (TPP) microfabrication to produce micron scale, three-dimensional hydrogel actuators [49]. PNIPAM exhibited a reversible, lower critical solution temperature (LCST) phase transition, while Fe_3O_4 nanoparticles served as potent photothermal agents, under near-infrared laser irradiation, they absorbed light and converted it to heat, triggering PNIPAM contraction and thus light-driven deformation with excellent thermal stability. Li et al. fabricated an optical-responsive hydrogel by incorporating a water-soluble spiropyran photo-switch bearing sulfonate groups (Fig. 4(c)) [50]. Under visible light irradiation, the sulfonate functionalized spiropyran within the hydrogel network isomerized to its merocyanine form, thereby increasing the net charge density. This charge increase enhanced the material's hydrophilicity and generated electrostatic repulsion that inhibited hydrophobic aggregation. As a result, the heightened hydrophilicity promoted water diffusion into the hydrogel network, causing volumetric swelling and bending of the gel away from the light source.

Light-responsive materials enable rapid, precise actuation via photothermal or photochemical mechanisms. Modulating irradiation parameters, such as wavelength, intensity, and polarization allow for high spatiotemporal control. While visible or NIR-responsive systems offer low toxicity for environmental and microfluidic applications, limited penetration and safety concerns restrict their use in deep tissues or opaque media.

2.3 Electric-responsive materials for actuation

Electric-responsive soft actuators are driven by virtue of the strain generated when the martials are electrically actuated. Various soft materials are employed to fabricate electric-responsive soft actuators, including electrothermally driven materials (e.g., shape memory alloys (SMA), dielectric elastomer actuators (DEAs)) [51, 52], and ionic actuators, such as hydrogels [53]. By emulating biological electrical signals, different voltages can be simultaneously applied to distinct regions of the electric-responsive soft actuators, thereby enabling them to execute complex, programmable actions [54].

2.3.1 *Electric-responsive dielectric elastomer actuators*

Conventional dielectric elastomer actuators typically comprise a dielectric elastomer membrane sandwiched between two soft electrodes. The fundamental mechanism driving deformation under an electric field is the generation of Maxwell stress. When a voltage is applied across the electrodes, opposite charges on the electrode surfaces attract one another, creating an electrostatic force. This force transmits through the elastomer membrane, producing compressive stress in the thickness direction and tensile stress in the planar directions. In actuators with tailored geometries, the Maxwell-stress-induced area expansion and thickness contraction are converted into bending, uniaxial extension, or more complex three-dimensional deformations. The speed and amplitude of these deformations depended on both the applied voltage and the driving frequency.

Various optimization strategies have been proposed to improve the electric-driving performance of actuator [55, 56]. Current research on dielectric elastomer actuators includes a focus on the development of novel dielectric materials with high sensitivity. Adeli et al. reported a muscle-inspired dielectric elastomer fabricated from crosslinked brush polymers. The brush polymers consisted of a polymer backbone with side chains, which extended the backbone and reduced entanglement. Due to the plasticizing effect of the side chains and reduced chain entanglement, the brush polymer material remained soft under small strains. In contrast, strain-induced stiffening increased the elastic modulus at large deformations, thereby enabling actuation at low voltages while preventing the onset of electromechanical instability (EMI) under high voltages. Tang et al. reported a self-contained soft electro-fluidic actuator (SEFA) [57]. As shown in Fig. 5(a), it utilizes a specially designed electro-conjugate fluid (ECF) instead of the solid dielectric medium within traditional dielectric elastomers, driving the deformation of the external elastomer through the electric-responsive fluid inside the actuator, directly converting electrical energy into mechanical energy. Compared to the response speed of traditional dielectric elastomers, the highly compact SEFA integrates ECF jet pumps, channels, reservoirs, and actuators, achieving a faster response speed.

2.3.2 *Electrothermal-responsive materials*

Electrothermal-driven soft actuator materials achieve deformation via resistive (Joule) heating and generally consist of a conductive component and a thermos-responsive segment. Deformation in these materials is driven by the electrothermal effect: When an electric current passes through the conductive element, resistive heating generates thermal energy, which in turn raises the temperature of the thermos-responsive material serving as the actuator's active element.

Recent efforts concentrate on the materials and structure design for high electrothermal conversion efficiency and multifunctionality. Patel et al. developed a highly dynamic bistable soft actuator comprising a 3D-printed elastomeric frame with embedded SMA coils and a pre-stretched membrane sandwiched between the frames [58]. The actuator's core driving mechanism was the thermal response of the SMA coils, inducing a phase transformation that drove rapid, bistable shape change of actuator. Liu et al. developed a rewritable, electrically controlled liquid crystal actuator using PEDOT:PSS as a conductive layer to mimic biological motion [52]. The hydrophilic PEDOT:PSS coating dispersed easily in water and could be removed with water or ethanol, enabling rewritable electrical pathways via spin-coating without damaging the substrate. This reconfigurable design allowed distinct actuation modes. As shown in Fig. 5(b), current passing through PEDOT:PSS generated Joule heating, and when the temperature exceeded the liquid crystal elastomer's phase-transition point, reversible thermal actuation was triggered, deforming the LCE.

2.3.3 *Electric-responsive ionic materials*

Ionic actuators represent another important class of electrically responsive soft actuators, typically comprising hydrogel matrices or ionomer polymers [59–61]. Under an applied electric field, deformation arises primarily from migration and redistribution of mobile ions within the material. When these actuators are immersed in an electrolyte solution and a voltage applied, cations and anions migrate toward oppositely charged electrodes. The directional movement and accumulation of ions near the electrodes generated ion-concentration and electric field gradients within the actuator. These nonuniform ion distributions produced localized stresses or pressure differentials, driving solvent flux or localized swelling and deswelling, which in turn induced macroscopic deformation of the actuator.

For example, Shin et al. developed an electrically stimulated soft

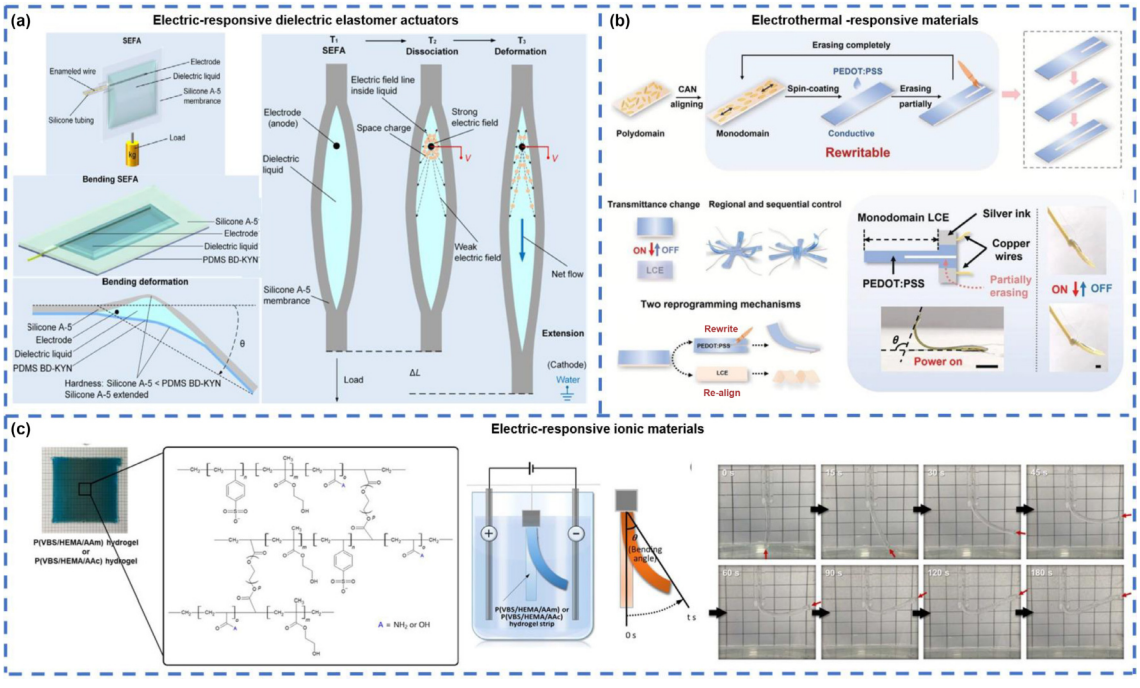

Figure 5 Electric-responsive materials for actuation. (a) Electro fluidic dielectric elastomer material. Reproduced with permission from Ref. [57], © Tang, W. et al. 2021. (b) Electrothermal responsive material. Reproduced with permission from Ref. [52], © Wiley-VCH GmbH 2023. (c) Electric-responsive ionic hydrogel material. Reproduced with permission from Ref. [6], © American Chemical Society 2021.

hydrogel actuator that exhibited rapid, flexible folding under low electric fields [6]. As shown in Fig. 5(c), when an electric field was applied, negatively charged fixed groups in the polymer network repelled mobile anions toward the anode while cations accumulated at the cathode, increased water ingress at the anode caused local swelling and simultaneous cathode-side contraction. This asymmetric swelling–deswelling generated a bending force toward the contracting side, and the bending direction could be tuned by adjusting the hydrogel's aspect ratio.

The recent research progress of ionic actuators mainly includes doping high-performance organic materials into flexible substrates to prepare ionic actuators with better performance and faster reaction speed. Kotal et al. reported a bionic muscle based on a three-dimensional graphitic carbon nitride (GCN)-nitrogen-doped graphene (NG) heterostructure electrode that enhanced the actuator's electrical responsiveness and mechanical performance [62]. The 3D GCN-NG heterostructure was deposited onto a PEDOT-based soft electrode, its nitrogen-rich composition and porous morphology enhanced electrical responsiveness by approximately fourfold, markedly improving mechanical performance. Because cations and anions typically differed in molecular size, they accumulated unequally near the electrodes, causing asymmetric local volume contraction and expansion. These heterogeneous volumetric changes generated internal stresses that induced macroscopic bending of the actuator.

Electric-responsive materials directly convert electrical energy into mechanical work, offering fast response times and precise, signal-dependent actuation for artificial muscles and sensors. While biocompatible, their utility is often hampered by high operating voltages, exceeding hundreds of volts, which increase the risk of dielectric breakdown and reduce device reliability.

2.4 Thermal-responsive materials for actuation

Thermal-responsive materials function primarily based on their intrinsic thermal effects. When subjected to a sufficient temperature change, their physical properties or spatial structures undergo modifications, leading to deformation. Several thermo-responsive soft actuator design strategies have been reported, which are mainly categorized into liquid crystal elastomers [63, 64], hydrogels [65–68], and composite elastomers featuring bilayer or multilayer structures [69–72].

2.4.1 Thermal-responsive liquid crystal elastomer materials

Thermal-responsive LCEs are composed of soft polymer backbones linked to rigid, liquid-crystalline mesogenic units (Fig. 6(a)). At temperatures below the phase-transition threshold, low thermal energy allows intermolecular forces to maintain a high degree of mesogen alignment along a preferred director, preserving a stable anisotropic state. Upon heating past the LCE's phase-transition temperature, the mesogenic order is disrupted as the system enters an isotropic phase. This loss of orientational order altered the average alignment angles of the mesogens, producing a macroscopic shape change in the material.

The development of thermal-responsive liquid crystal elastomers includes the structure design of materials that can effectively improve the thermal sensitivity. Zhang et al. developed a thermally

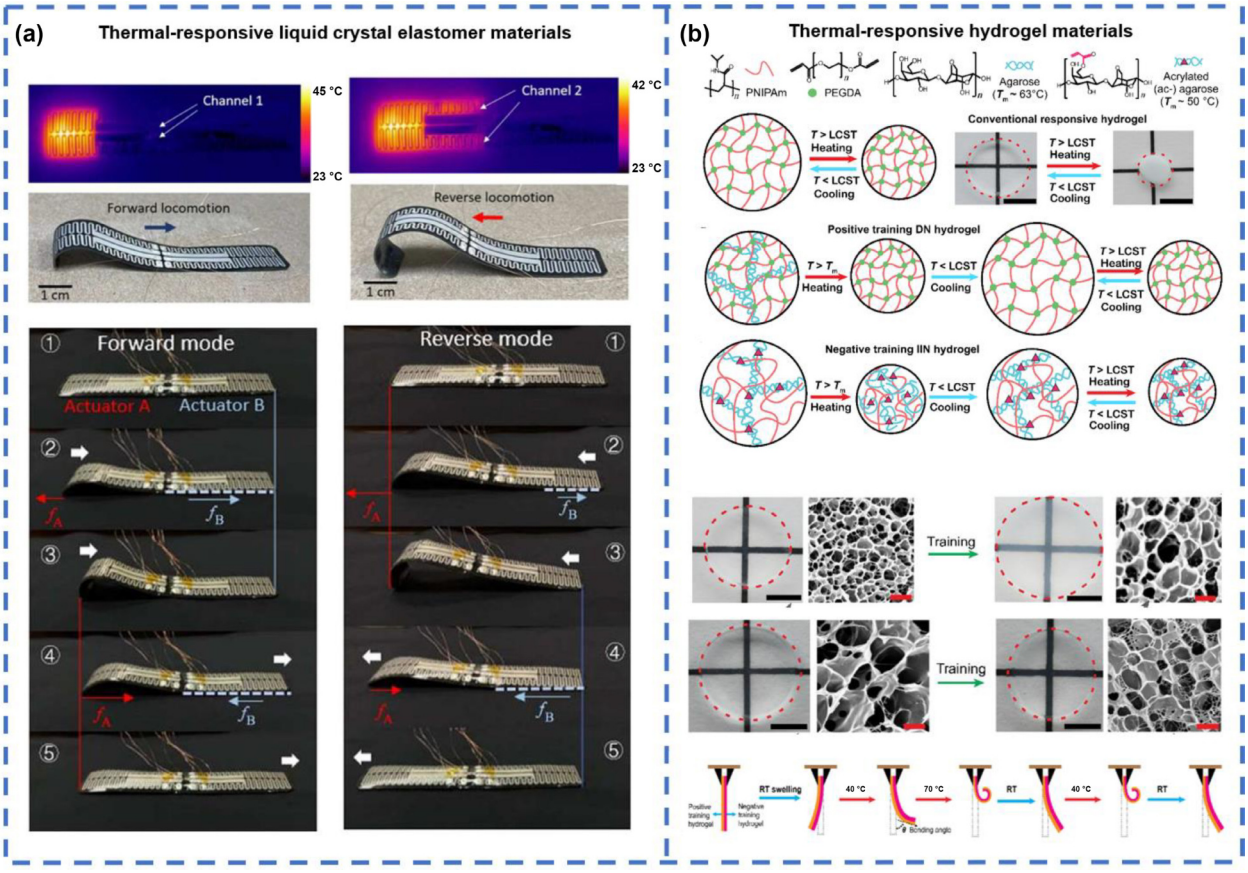

Figure 6 Thermal-responsive materials for actuation. (a) Thermal-responsive hydrogel material. Reproduced with permission from Ref. [17], © Wu, S. et al. 2023. (b) Thermal-responsive liquid crystal elastomer material. Reproduced with permission from Ref. [73], © Hu, S. M. et al. 2023.

responsive soft actuator composed of LCE foam fabricated by a salt-templating method that produced omnidirectional bending under unilateral heating. The foam's low thermal conductivity generated a through-thickness temperature gradient. When heated above its transition temperature, the LCE entered the isotropic phase, and mesogen alignment was disrupted. This caused contraction along the original alignment and expansion perpendicular to it, creating a contraction gradient that bent the foam toward the heat source, relocating the source re-established the gradient and induced bending in new directions.

2.4.2 *Thermal-responsive hydrogel materials*

Thermo-responsive hydrogel actuators typically possess a LCST. When the temperature exceeded the LCST, the temperature-sensitive polymer chains within the hydrogel became hydrophobic, inducing dehydration, contraction, and reversible shape change. Conversely, below the LCST, the hydrogel absorbed water and swelled. This reversible dehydration-rehydration cycle results in a macroscopically observable shrinkage–expansion process, making hydrogels suitable for thermal–responsive applications.

The performance of thermal-responsive hydrogels can be adjusted by doping them with different compounds [74–76]. Building on this, polymer hydrogels featuring interpenetrating-network (IPN) or dual-network (DN) architectures demonstrated superior thermos-responsive performance. Hu et al. reported a trainable hydrogel of two thermosensitive polymers that exhibited a reversible negative-training effect by temperature-controlled melting and reconstruction of an agarose network [18]. In the agarose/PNIPAM dual network (Fig. 6(b)), the PNIPAM phase collapsed above its LCST but its volumetric change was constrained by the relatively rigid agarose. When heated above both PNIPAM's LCST and the melting point of the acrylated agarose fibrils, PNIPAM shrank while the agarose microfibrils melted. On subsequent cooling, the acrylated agarose re-gelled within the reduced volume, increasing the density of physical crosslinks, this reinforced agarose network further restricted swelling, produced an overall size decrease after thermal cycling, and thereby enabled the reversible negative-training effect.

Another design strategy for thermos-responsive hydrogel is based on bilayer or multilayer constructs, whose core mechanism for thermally induced deformation lay in exploiting the differential responses of constituent materials to temperature changes. Kobayashi et al. reported a bilayer hydrogel actuator, fabricated by photolithography, that combined a thermal-responsive, highly swellable P(OEGMA-DSDMA) active layer with a low-swelling P(AAm-BAC) passive layer [77]. The active P(OEGMA-DSDMA) layer had a relatively low LCST and thus underwent pronounced swelling or shrinkage with temperature, which afforded the actuator high operational efficiency. The LCST difference between the layers further increased actuating sensitivity. Upon temperature change, the active layer's large volume variation and the bonded passive layer's minimal response generated internal stress in the bilayer, producing bending deformation of the actuator.

Thermal-responsive materials undergo significant volumetric changes triggered by temperature, which can be tuned via composition for localized biomedical tasks like drug delivery. Although many such systems are biocompatible materials, their reliance on heat conduction causes slow recovery and limits high-frequency cyclic operation.

2.5 Chemical-responsive materials for actuation

2.5.1 *pH-responsive materials*

Chemically responsive materials exhibit specific response mechanisms to particular chemical stimuli, triggering alterations in their spatial structures or inducing the breaking and reorganization of chemical bonds between polymer chains [78, 79]. These characteristics enable them to reversibly respond to external chemical stimuli, such as pH changes [80–86], ionic strength variations [87], or the presence of specific chemical substances [88]. Chemically responsive materials based on polymer networks, particularly hydrogels, have attracted significant research interest. The popularity of hydrogels stems from their high water-absorption capacity and the sensitivity of their network structure and solvent interactions to external stimuli. The polymer chains typically carry functional groups that respond to chemical cues.

To enhance responsiveness, functional components are often added to the polymer matrix or introduced through chemical modification. Kang et al. reported a pH-responsive hydrogel actuator driven by reversible borate-ester bonds between polyvinyl alcohol (PVA) and borate, with carbon quantum dots (CDs) contributing to surface-layer formation [89]. The PVA-polyacrylamide network exhibited dynamic PVA-borate ester crosslinks (Fig. 7(a)). At pH approximately equal to 8.5, the hydrogel underwent a reversible gel–sol transition: A sol layer containing free borate/boric acid and CDs formed on the surface, inducing actuation. When pH fell below the pKa of boric acid, the borate esters cleaved and the gel converted to a sol. Adding base re-ionized boric acid reformed the borate esters and restored the gel state. The incorporation of carbon quantum dots improved the lubricity and mechanical properties of the hydrogel and made the sol layer uniquely observable.

2.5.2 *Humidity-responsive materials*

Humidity-driven soft actuators often incorporate materials with varying water absorption capacities, leading to differential swelling and unbalanced deformation across the material's surface, thereby generating the driving force for movement. Alternatively, asymmetric exposure of water-absorbing materials to moisture can similarly induce directional deformation [90].

In recent years, the research on humidity-responsive materials has mainly focused on organic materials with great hygroscopic properties, mainly carbon materials, such as graphene oxide (GO) and MXene. Weng et al. reported a mussel-inspired, humidity-responsive soft actuator based on polydopamine-modified MXene that produced controlled bending under moisture gradients [8]. MXene films can adsorb large amounts of water and swell rapidly. By incorporating asymmetry—material, structural, or moisture gradients—programmable deformation is enabled. As shown in Fig. 7(b), preferential wetting of one face created a water-content gradient whose resulting internal stress bent the actuator toward the drier side, yielding humidity-responsive actuation.

Chemical-responsive materials undergo programmable deformation and functional switching via pH or humidity stimuli. Molecular-level engineering of responsive motifs and cross-linking enables complex spatial movements and intrinsic sensing, ideal for underwater and environmental monitoring. However, slow diffusion and reaction kinetics typically impede rapid, repeatable cycling.

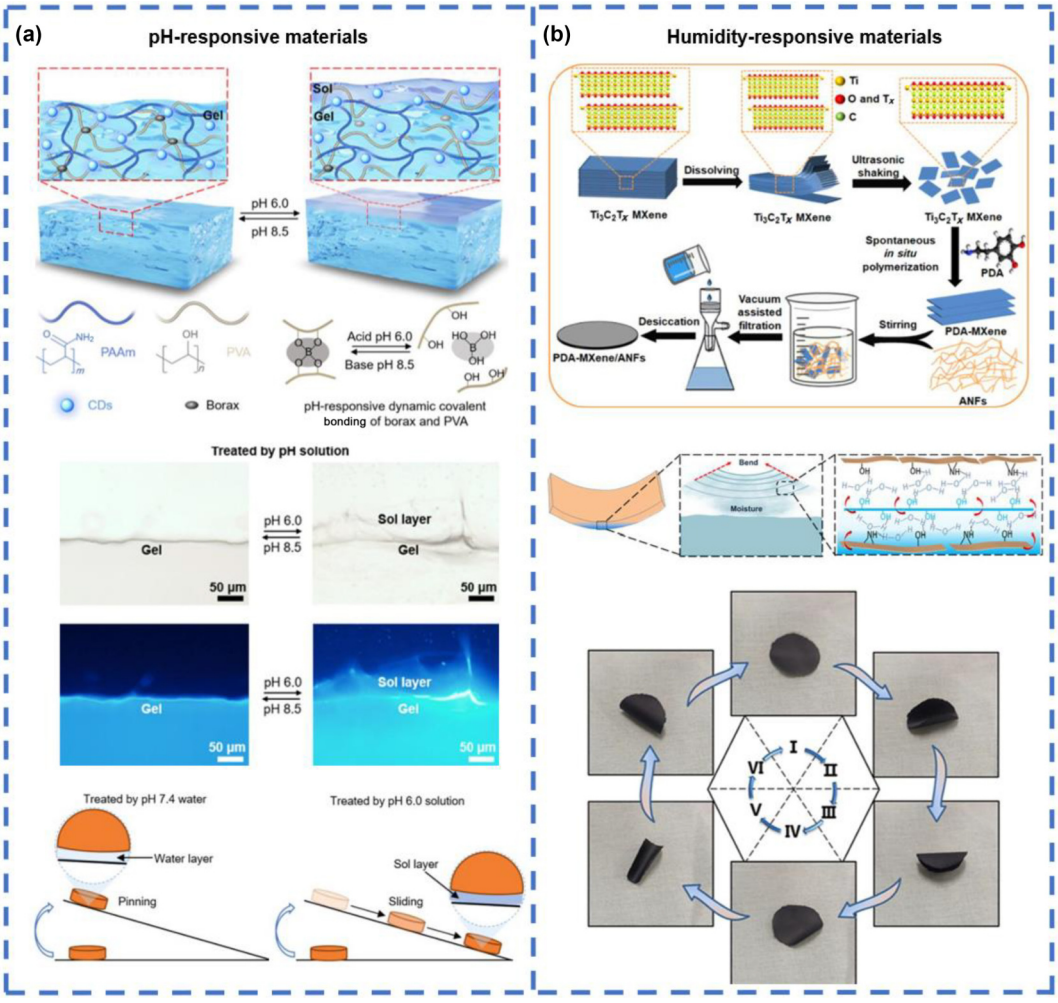

Figure 7 Chemical-responsive and humidity-responsive materials for actuation. (a) PH-responsive hydrogel material. Reproduced with permission from Ref. [89], © Elsevier B.V. on behalf of Chinese Chemical Society and Institute of Materia Medica, Chinese Academy of Medical Sciences 2024. (b) Humidity-responsive MXene-based material. Reproduced with permission from Ref. [8], © American Chemical Society 2024.

2.6 Multi-responsive materials for actuation

To realize multi-responsivity in soft actuators, various material design strategies have been developed, which can be generally categorized into three main approaches: utilizing intrinsically multi-responsive materials, assembling multiple single-responsive components into hybrid structures, and integrating different response mechanisms through chemical modification. These strategies enable actuators to respond to diverse external stimuli such as heat, light, electricity, magnetism, and humidity, thereby enhancing their adaptability and functionality in complex environments.

Some organic materials (graphene oxide [91, 92] and carbon nanotubes [93]) inherently possess the ability to respond to multiple stimuli, enabling the fabrication of multi-responsive materials from a single-layer material. Zhang et al. reported a multi-responsive soft actuator based on a photo-crosslinked poly(ε-caprolactone) (cPCL) film into which CNTs were embedded on the surface [94]. The actuator combined good electrical conductivity for electrical driving with preserved thermally induced actuation. Under thermal stimulation, crystallization and melting of the actuation domains induced shape change. Simultaneously, when an electric field was applied, current flowing through the CNT conductive layer generated Joule heating, which raised the surface temperature and triggered crystallization/melting of PCL microcrystals, thereby enabling reversible shape transformations.

An alternative fabrication strategy involves physically bonding multiple single-responsive materials, such as SMAs [95], metal nanowires [96], liquid crystal elastomers (Fig. 8(a) [97–100]) and hydrogels (Fig. 8(b) [101–105]) to produce composite, multi-responsive materials. Yin et al. reported a multi-responsive film material made from a biaxially stretched polypropylene (BOPP) composite film combined with conductive polyethylene terephthalate (PET) and produced through lamination techniques [106]. The resulting soft robots showed good responsiveness to various stimuli, including magnetic, electrical, optical, and thermal stimuli. Maiz-Fernández et al. reported a multi-responsive hydrogel soft robot doped with alginate and magnetic nanoparticles [107]. The alginate in a calcium ion environment provides the soft robot with electrical responsiveness and good mechanical stability. At the same time, the porous structure of alginate enhances the hydrogel's adsorption capacity, allowing for better incorporation of magnetic nanoparticles, which gives it good magnetic responsiveness.

Furthermore, by chemical compounding, materials with different response modalities could be integrated to form new substances with multi-responsive capabilities. Figure 8(c) presents a soft

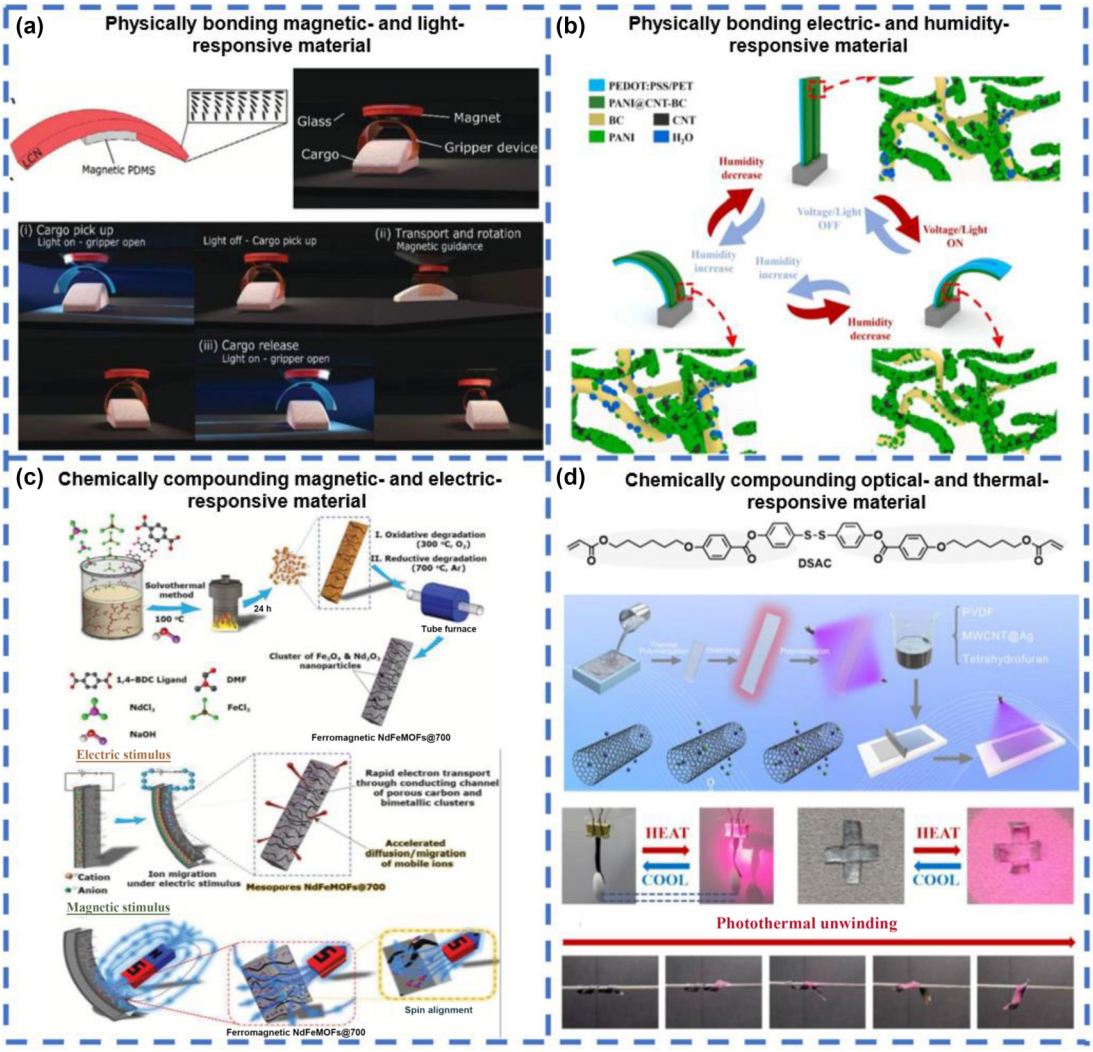

Figure 8 Multi-responsive materials for actuation. (a) Magnetic- and light-responsive actuator by physically bonding two single-responsive layers. Reproduced with permission from Ref. [97], © da Cunha, M. P. et al. 2019. (b) Electric- and humidity-responsive actuator by physically bonding multiple single-responsive hydrogels and carbon materials. Reproduced with permission from Ref. [101], © Elsevier B.V. 2022. (c) Magnetic- and electric-responsive actuator by chemically compounding metals and metal oxides. Reproduced with permission from Ref. [9], © Wiley-VCH GmbH 2023. (d) Optical- and thermal-responsive actuator by chemically compounding LCE and CTNs. Reproduced with permission from Ref. [108], © Elsevier B.V. 2024.

actuator based on a ferromagnetic bimetallic organic framework with magnetic and electric responses [9]. The specially designed NdFeMOFs active electrode material contains graphite structures of metals and oxides of Nd and Fe, demonstrating excellent electromagnetic properties. Zhang et al. reported a self-healing, multimodal soft actuator that combined a disulfide-containing LCE with a photothermal-conductive functional layer [108]. As shown in Fig. 8(d), they designed an aromatic DSAC molecule bearing disulfide bonds to provide self-healing and prepared a functional coating by reacting hydroxylated multi-walled carbon nanotubes (OH-MWCNTs) with acryloyl chloride, which imparted photothermal and electrical conductivity. The actuator achieved multimodal motion through the LCE's thermally induced phase transition and the functional layer's energy conversion: Heating above the LCE transition temperature caused anisotropic contraction and bending, while near-infrared or electrical stimulation generated localized heat that drove similar deformation in a controllable and repeatable manner.

Multi-responsive materials integrate multiple actuation mechanisms to overcome the constraints of single-mode systems. This synergy enhances adaptability, deformation amplitude, and response speed, facilitating complex biomimetic motions. Nevertheless, their multilayered or laminated architectures may complicate structural optimization and increase fabrication costs.

3 Bioinspired locomotion of small-scale soft robots

Locomotion is a fundamental capability that enables animals to interact with their environment to search for food, escape from predators, and explore habitats. Over the course of evolution, organisms across different taxon have developed a wide variety of movement strategies suited to their living environments. These include legged or limbless crawling, jumping, swimming, and flying, among others. Understanding and abstracting the physical principles behind such biological movements have inspired extensive research into small-scale soft robotic systems (Table 2), where mimicking these biological strategies offers unique

advantages in adaptability, efficiency, and environmental interaction.

3.1 Crawling motion

Crawling is a mode of locomotion used by most invertebrates, such as soft-bodied animals and arthropods, as well as reptiles. The key to crawling lies in the cooperative action between frictional or adhesive forces and the environment. These frictional or adhesive interactions typically require anisotropy. Under external environmental factors (such as applied magnetic fields [109], electric fields [110, 111], and light [112]), soft robots can perform friction-based crawling movements. Crawling soft robots benefit from their mobility and good environmental adaptability, making them suitable for tasks like detection and exploration in confined spaces [113–118]. Recent researches of soft crawling robots mainly focus on inchworm and caterpillar crawling locomotion.

Inchworm crawling locomotion is a discrete, anchor-and-reach locomotor cycle in which the animal first fixes its anterior legs, contracts longitudinal muscles to draw the posterior body forward into a U-shaped loop, plants the posterior prolegs as a new anchor, then extends the anterior body forward to complete the step. Because these larvae lack middle abdominal prolegs, the motion is organized as repeated "anchor–contract–anchor–extend" cycles, large stride lengths on narrow substrates and good grip with minimal muscular work are permitted. Current research focuses on mimicking the inchworm's movement while using different materials and drive methods to improve its efficiency. Liu et al. reported an electric-responsive crawling soft robot powered by mechanical energy [119]. The robot consists of a flexible acrylic frame and dielectric elastomer films, with two pairs of triboelectric adhesive feet (TAF) that utilize a triboelectric nanogenerator (TENG) to provide power, as shown in Fig. 9(a). By controlling the voltage released from the control module, the collaborative movement between the soft body and the TAF is managed, allowing the soft robot to crawl on different substrates. Jiao et al. reported a biomimetic worm robot based on the piezoelectric effect, constructed from piezoelectric rubber and a flexible substrate [12]. When the robot is inflated by a pump, its asymmetrical body design ensures it can bend. The piezoelectric rubber generates electrical signals when compressed, and an external circuit controls the pump to stop inflation, allowing it to enter a deflation state and complete a single crawling action. The piezoelectric effect enables the robot to rapidly complete multiple inflation-deflation cycles in a short time, achieving precise, quick, continuous self-driven crawling.

Caterpillar crawling locomotion is achieved by sequential contraction and relaxation of body segments or foot muscles that produce traveling compression. In this mode, phase-shifted muscular activity advances a localized shortening and elongation wave along the body or foot, local anchoring structures (setae, prolegs) or pedal mucus prevent backsliding and convert the wave into net forward displacement. Rogóz et al. reported an LCE-based, light-responsive soft caterpillar robot, as shown in Fig. 9(b) [120]. Inspired by the traveling-wave deformation mechanism of caterpillars, they patterned molecular alignment so that the frictional regions contracted along the direction of friction, propulsion derived from friction between LCE strips and the substrate, while the non-illuminated regions in contact with the ground provided support. The deformed regions lifted and advanced, establishing asymmetric friction and producing a propagating wave of local bending from tail to head.

Crawling robots utilize compact structures and high surface contact to navigate narrow or curved environments. While spatially adaptable, their efficacy depends heavily on interfacial friction and the material's elastic recovery rate. Consequently, crawling is typically low-speed and requires sophisticated sensing for complex feedback control.

3.2 Legged motion

The evolution of legs endowed animals with the ability to achieve large-scale displacement, adjusting their stride length and posture,

Table 2 Selective hydrogenation of FAL over different catalysts

Locomotion modes	Advantages	Disadvantages	Material	Bioinspiration	Speed	Size	Locomotion medium	Ref.
Legged	Adaptability to unstructured terrain, passive compliance and impact resistance	High degrees of freedom and high algorithm complexity, lower motion efficiency ratio than wheeled mechanisms	IP-DIP	Spider	N/A	200 μm	aerial	[126]
			PDMS	Ladybird	25 mm/min	115 mm	aerial	[133]
			PA2200	Turtle	20 mm/s	150 mm	aerial	[134]
Crawling	High conformal interface contact, compact structure with extremely high space utilization, strong stability within constrained spaces	Low moving speed, performance is highly dependent on interfacial friction/adhesion, susceptible to surface contamination	DE/PET/PTFE/CNT	Inchworm	11.61 mm/s	43 mm	aerial	[116]
			PI/PDMS	Caterpillar	2.38 mm/s	70 mm	aerial	[110]
			PI/GO/Ag	Inchworm	8.1 mm/min	20 mm	aerial	[111]
Jumping	Instantaneous large-span displacement, great vertical spatial accessibility	Challenging landing impact dissipation and air attitude control, limited load capacity and materials are prone to fatigue failure	NI/TI/SMA	Walk strider	1.5 m/s	15 mm	Aquatic-aerial	[149]
			$Ti_3C_2T_x$ Mxene/PDMS/PI	Steinernema carpocapsae	92.3 mm/s	20 mm	aerial	[152]
			NdFeB/PDMS	Walk strider	40 cm/s	25 mm	Aquatic-aerial	[11]
Swimming	High maneuverability in three-dimensional space, efficient propulsion achieved through flow field coupling	Difficult maintaining attitude in strong turbulence or unsteady flow fields, strong coupling contradiction between velocity and effective load	PNIPAM/CNT	Fish	60 cm/s	30 mm	Aquatic	[159]
			PNIPAM/CNT	Jellyfish	3.37 mm/s	10 mm	Aquatic	[160]
			GO/PDMS	Whirligig beetle	20 mm/min	45 mm	Aquatic	[170]
Flying	High energy autonomy (passive), agility and spatial coverage (active)	Uncontrollable movement trajectory(passive), high power consumption density and limited load capacity(active)	PU/CNT/Parylene C	Bee	8 cm/s	20 mm	aerial	[178]
			PVA/PI	Dandelion	10 cm/s	10 mm	aerial	[179]

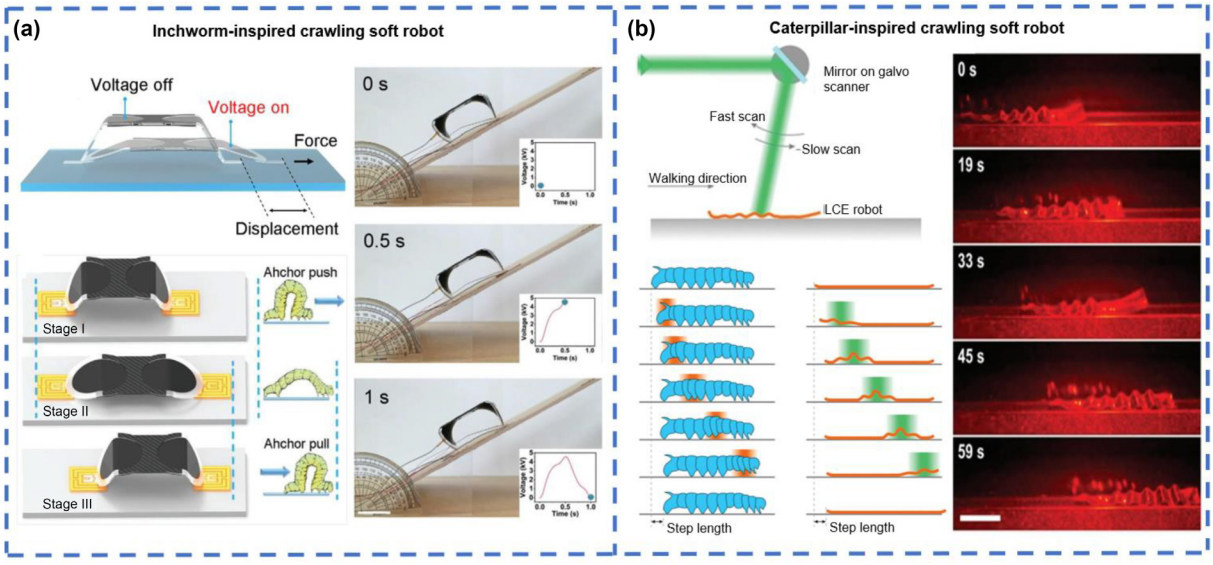

Figure 9 Crawling locomotion of small-scale soft robots. (a) Inchworm-inspired crawling locomotion. Reproduced with permission from Ref. [119], © Wiley-VCH GmbH 2021. (b) Caterpillar-inspired crawling locomotion. Reproduced with permission from Ref. [12], © WILEY-VCH Verlag GmbH & Co. KGaA, Weinheim 2016.

and thus navigating complex terrain [121–126]. In the field of soft robotics, researches mainly focus on quadrupedal walking because it balances stability with precise control over speed and direction. Quadrupedal walking is achieved by alternating cyclic stance and swing phases of four limbs with organized interlimb phasing that maintains a moving support polygon beneath the body, and can be seen in horses, dogs, lizards and so on. At slow speeds, many quadrupeds use lateral or single-footed walks in which three feet remain in contact with the ground to maximize static stability. At intermediate speeds, they typically adopt diagonal couplets and at high speeds shift to asymmetrical gaits that introduce aerial phases [127–131].

One method of achieving quadrupedal locomotion is periodically alternating the support and swing phases of two pairs of legs, generating reaction forces that propel the body forward [132–138]. Huang et al. reported a magnetically driven quadrupedal soft robot [139]. As shown in Fig. 10(a), the robot consisted of a main body and four magnetized flexible legs. When the robot was subjected to a conical magnetic field formed by the superposition of a right-handed rotating magnetic field and a static magnetic field, alternating deformation of the four legs could be controlled by adjusting the magnetic-field parameters, thereby realizing locomotion.

Another common approach to achieve quadrupedal walking is cyclically driving leg swinging through bending and straightening motions to generate forward propulsion. Atia et al. reported a modular, block-based reconfigurable soft robot that was assembled by connecting distinct functional modules and possessed multiple capabilities, allowing it to adapt to different environments and interact with complex objects [10]. As shown in Fig. 10(b), when the robotic legs received periodic electrical current, the DEA film within them underwent deformation, causing the legs to bend. Upon current cessation, the legs straightened, thereby generating driving force.

Legged motion offers superior stability and terrain adaptability for exploration and search-and-rescue in irregular environments. However, the necessity for multi-limb coordination and posture computation increases control complexity and energy consumption, often resulting in lower locomotion speeds than simpler structural systems.

3.3 Jumping motion

In nature, jumping is an efficient locomotion strategy commonly employed by animals to navigate cluttered environments and rugged terrains. This mode of movement enables animals to capture prey, evade predators, and surmount large obstacles. During jumping, small animals such as fleas, leafhoppers, springtails, and some orthopteran insects often slowly store muscle-generated energy in elastic proteins or specialized spring-like organs and then rapidly release it during takeoff to achieve very high instantaneous power. By contrast, medium or large-scale animals generate takeoff velocity by direct work of limb extensor muscles transmitted through joints and lever systems [140–147].

One approach for soft robots to achieve jumping involves energy storage, where the kinetic energy storage components are designed to store energy while maintaining excellent controllability, thereby achieving high-quality jumping motions [148–151]. Wang et al. proposed a small, amphibious, magnetically responsive soft jumping robot capable of programmable jumps in both aquatic and terrestrial environments [11]. As shown in Fig. 11(a), when an initial magnetic field was applied, its legs were magnetized to convert magnetic energy into mechanical elastic potential energy, compressed and stored elastic potential energy, the subsequent release of that energy produced the jump. Upon landing, the elastic torque reversed and the magnetic torque was increased to replenish the robot's potential energy. Xu et al. introduced a light-responsive soft jumping robot based on MXene, inspired by insect larvae [152]. This robot curled into a ring-locking structure under dark conditions to store kinetic energy for jumping actions. When exposed to light, the locking structure opened due to the photothermal properties of MXene, releasing the stored elastic energy and allowing the soft robot to unfold and completed a rapid jump.

Another approach to achieve jumping is directly imparting kinetic energy to soft robots. Gorissen et al. reported a pneumatic

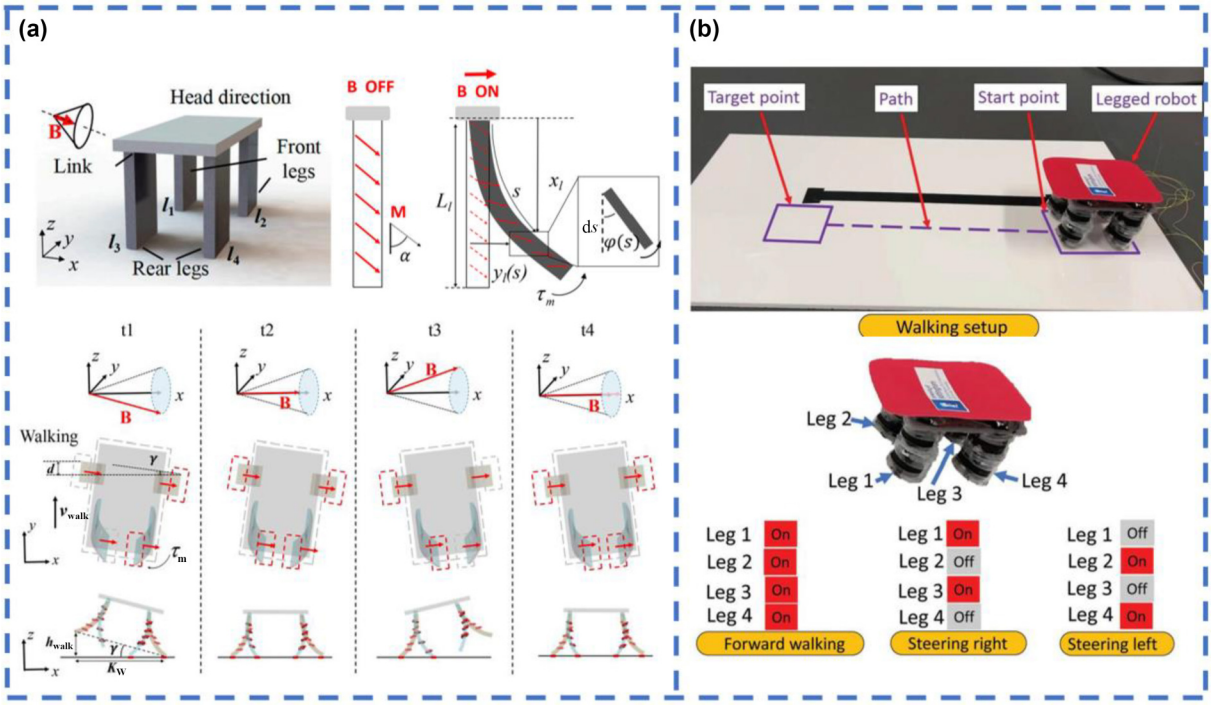

Figure 10 Legged locomotion of small-scale soft robots. (a) Legged locomotion achieved by alternating the support and swing phases of legs. Reproduced with permission from Ref. [139], © Huang, C. Y. et al. 2022. (b) Legged locomotion achieved by driving leg swinging through bending and straightening motions. Reproduced with permission from Ref. [10], © Atia, M. G. B. et al. 2022.

soft robot inspired by shells [153], which can achieve rapid jumping by injecting fluid into a rigid chamber, as shown in Fig. 11(b). By inflating the cavity to increase pressure, kinetic energy is released through rapid mechanical response once the cavity reaches its pressure limit point, enabling high-performance jumping.

Jumping robots leverage material-based energy storage and power amplification to rapidly traverse discontinuous or elevated terrains. Although this mode expands the accessible field of view and enhances agility, it demands high instantaneous power and robust landing buffering. Additionally, limited payload capacity and structural fatigue during repeated cycles remain key constraints.

3.4 Swimming motion

Swimming is a kind of locomotion in which a robot deforms its body to accelerate the surrounding fluid, generating reaction forces that propel the body. Its core principle is to produce rearward fluid momentum to generate forward thrust, while simultaneously overcoming fluid drag to sustain forward motion [154–161]. Several approaches are proposed to implement the swimming locomotion of small-scale robots, including jet propulsion, fin-body swimming, and hindlimb-powered swimming.

Jet propulsion is achieved by forcefully expelling water through siphon, and is utilized by animals such as octopuses, squids, nautiluses, and cuttlefish. They draw water into a flexible mantle cavity and rapidly contract circular mantle muscles to eject the fluid, producing a high-velocity jet that generates thrust. By orienting and rotating the siphon, they vector the jet to control direction, enabling rapid acceleration and agile maneuvering. This locomotor strategy is particularly advantageous for escape responses and quick reorientation in complex underwater environment [162–165]. Chen et al. reported an octopus-inspired, jet-propelled soft swimming robot that was driven by a folded-origami soft chamber coupled to soft biomimetic muscles made of LCE fibers [166]. When the robot was submerged, the LCE fibers were relaxed and the chamber filled with water. When the robot received an electrical signal, the LCE fibers heated and contracted, increasing the tensile load on the water-filled soft chamber. Once the tensile load exceeded a critical threshold, the chamber underwent instantaneous buckling and its volume rapidly contracted, ejecting a high-speed jet of water; the robot was propelled forward by the resulting reaction force, as shown in Fig. 12(a).

Fin-body swimming is commonly classified into body-and-caudal-fin (BCF) and median-and-paired-fin (MPF) modes. BCF propulsion is achieved by propagating lateral waves along the body axis and oscillating the caudal fin to accelerate water posteriorly and generate thrust. This strategy is used in various forms by carp, tuna and many sharks. MPF locomotion produces thrust by undulating or oscillating the pectoral or median fins and is characteristic of maneuvering and hovering swimmers such as wrasses, triggerfishes, and batoids like rays. Tian et al. designed a carp-inspired, three-dimensional free-swimming magnetic microrobot that exhibited high controllability, maneuverability, and environmental adaptability [167]. Under a periodically varying magnetic field, the robot's gradient modulus distribution generated spatially varying magnetic torques at different regions, driving periodic motion of the fin-like elements and producing a negative-buoyancy behavior, as shown in Fig. 12(b). Piazzoni et al. reported a soft swimming robot with a typical fish structure based on three-dimensional functional hydrogels [168]. An embedded, deformable, electric-responsive hydrogel serves as the driving module at the tail, imitating the oscillation of fish fins under low-pressure AC electric drive to realize swimming functionality.

Hindlimb-powered swimming is a locomotion method utilized by many amphibians such as frogs. In this method, amphibians use powerful hindlimb kicks for propulsion, illustrating different

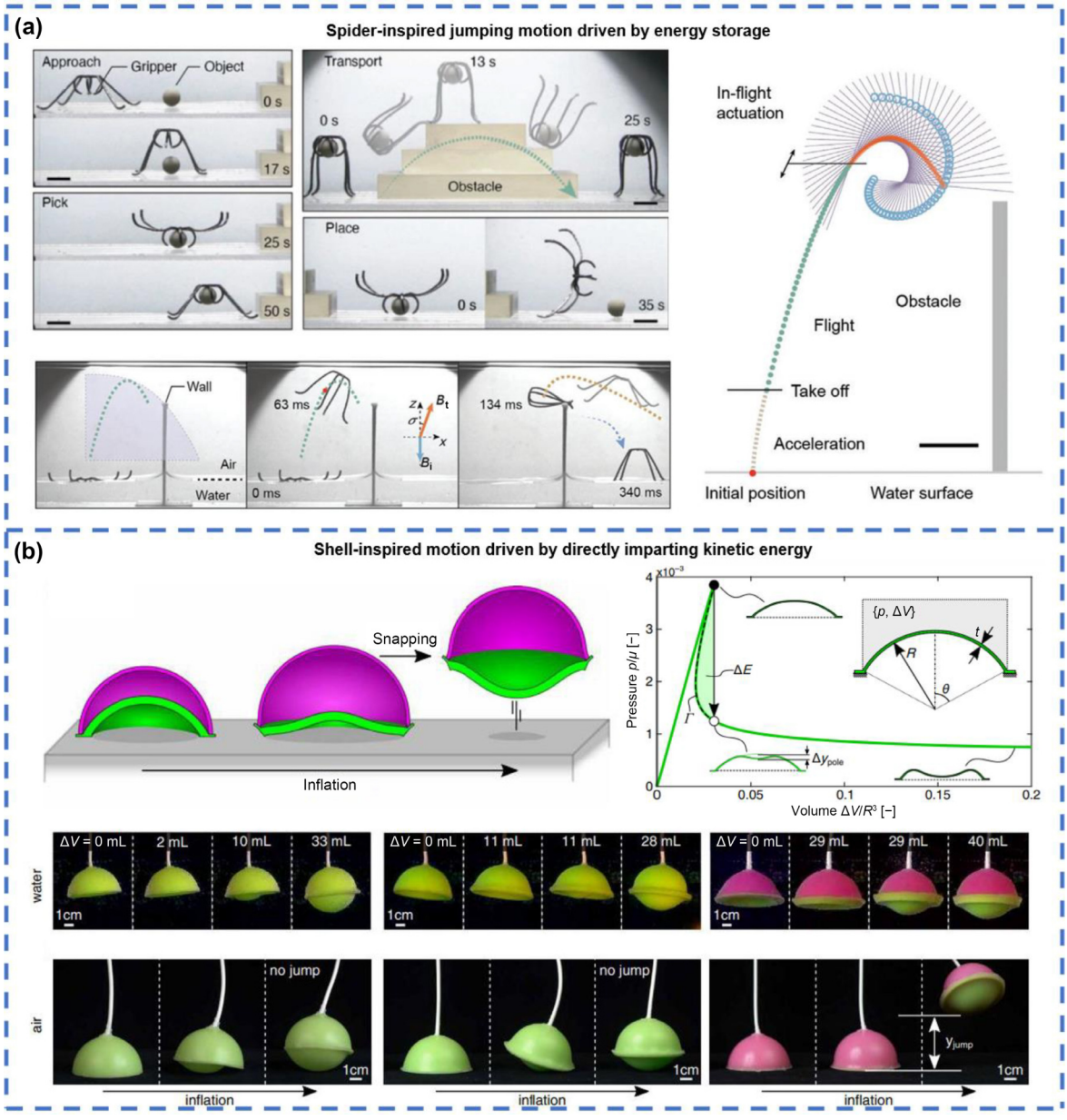

Figure 11 Jumping locomotion of small-scale soft robots. (a) Spider-inspired jumping motion driven by energy storage. Reproduced with permission from Ref. [11], © Wang, Y. B. et al. 2023. (b) Shell-inspired motion driven by directly imparting kinetic energy. Reproduced with permission from Ref. [153], © Gorissen, B. et al. 2020.

muscle-driven locomotor modes for underwater movement, providing inspiration for various soft swimming robots [169–173]. Soomro et al. reported a frog-inspired soft robot whose multilayer structure was composed of SMA and acrylonitrile–butadiene–styrene (ABS) materials [174]. As shown in Fig. 12(c), the frog-like soft robot's knee joints, head, and interdigital webbing were actuated by external electrical signals to control the robot, inducing hindlimb flexion, expansion of the interdigital webbing, hindlimb kicks, and inertial gliding. These actions generated thrust and exploited gliding to achieve long distance locomotion of robot.

Soft swimming robots utilize bioinspired designs for agile 3D maneuverability in complex aquatic or biological environments. While their compliance facilitates environmental monitoring and targeted drug delivery within narrow bodily cavities, maintaining stability in turbulent or high-shear flows remains challenging, and payload capacity is typically limited.

3.5 Flying motion

Flight is generally achieved by generating lift and thrust through flapping wings powered by muscles. This locomotion mode can be seen in animals like birds, bats, and locusts. They exploit unsteady aerodynamic mechanisms (e.g., wing rotation, leading-edge vortices, and wake capture) to create pressure differences across the wing surface that produce lift and forward thrust. Plants, by contrast, generate lift through their own hairs or pappus, winged seed coats, or thin-film aeolian sacs, enabling flight or suspension by harnessing wind power [175–178]. Thus, the bio-inspired flying locomotion of soft robots can be broadly categorized into two main types: passive flight mimicking plants and active flight mimicking animals.

Passive flight refers to the process by which organisms that lack their own means of locomotion are transported by wind or

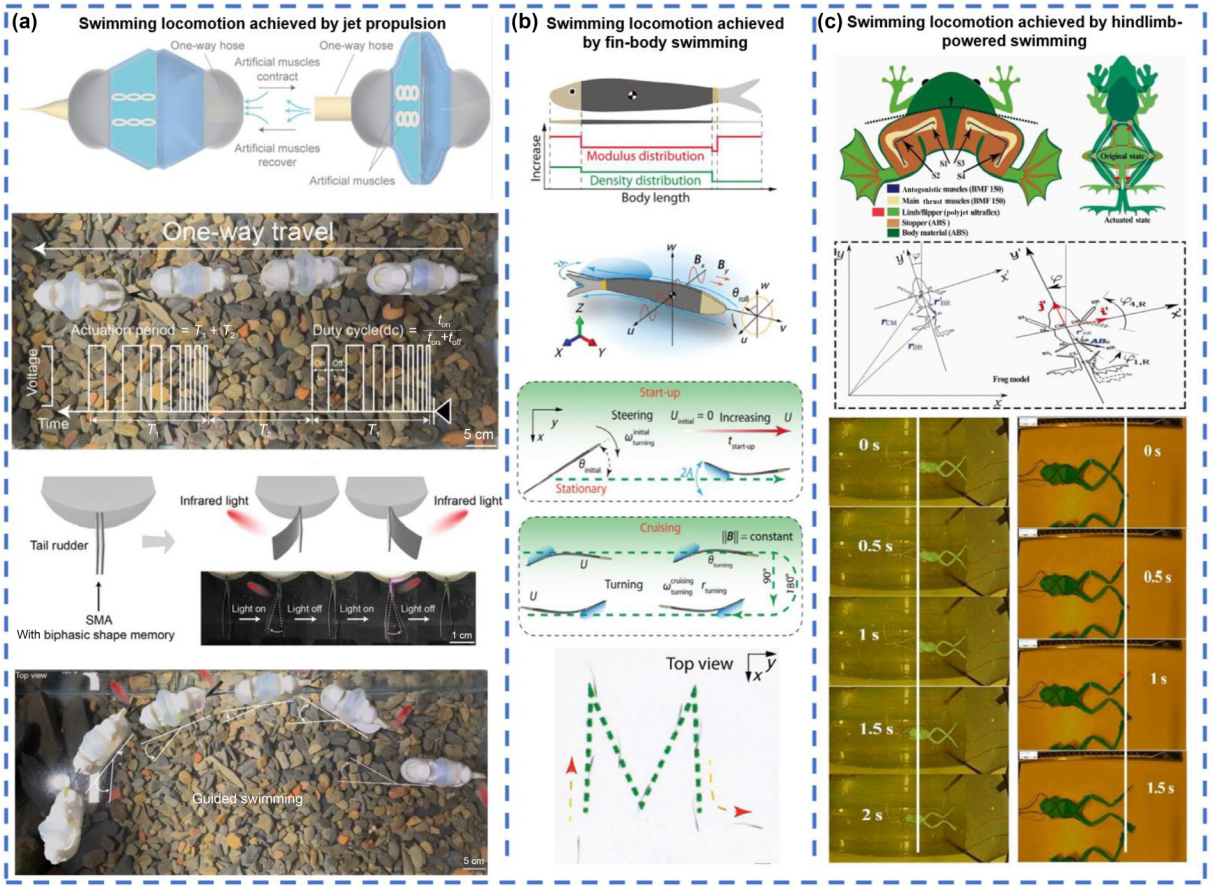

Figure 12 Swimming locomotion of small-scale soft robots. (a) Swimming locomotion achieved by jet propulsion. Reproduced with permission from Ref. [166], © Wiley-VCH GmbH 2025. (b) Swimming locomotion achieved by fin-body swimming. Reproduced with permission from Ref. [167], © Wiley-VCH GmbH 2024. (c) Swimming locomotion achieved by hindlimb-powered swimming. Reproduced with permission from Ref. [174], © Elsevier Ltd. 2021.

convection through interactions between their morphological structures and air currents, thereby achieving long-distance dispersal. This passive flight strategy is widely exhibited among plants, encompassing plumed pappi [179], autorotating winged samaras, minute dust-like seeds, and diaspores equipped with hairy or cottony appendages that extend aerial suspension times. Chen et al. fabricated a dandelion-inspired, light-driven microrobot built from a tubular, bistable soft-actuator film with glass fibers [180]. As shown in Fig. 13(a), upon infrared irradiation, an upward airflow formed, the photothermal effect of gold nanorods caused the robot's surface to expand, and the deployed glass fibers induced vortex-ring formation in the surrounding air, producing lift that enables flight.

Active flight is common among birds and some small insects and constitutes a refined mode of locomotion. It primarily relies on wings. Feathered wings in birds or membranous wings in insects, where contractions of the thoracic muscles generate lift and thrust, and wing motions effect attitude control during flight [181–185]. Chen et al. reported a bioinspired flying soft robot actuated by high-power-density elastic dielectrics [14, 186]. Specially designed elastomeric dielectric elements were mounted on a lightweight frame and coupled to a mechanical transmission (Fig. 13(b)). During takeoff, the elements underwent cyclic deformation under an applied electric field, driving wing flapping to generate sufficient lift for takeoff. By adjusting the drive voltages applied to individual actuators, the robot could achieve stable and controllable flight.

For flight locomotion, passive flight leverages environmental energy (wind) for long-duration sampling at low cost, though it lacks autonomous navigation. Conversely, active flight offers superior agility and precision for reconnaissance but requires high-frequency actuation and faces severe power-density and endurance constraints.

3.6 Multi-modal motion

Research in soft robotics increasingly targets multifunctional, multimodal platforms that can perform a range of tasks in complex environments. In particular, multimodal locomotion capability of small-scale soft robots are widely explored by designing the robot's composition and architecture to realize specialized responses to external stimuli [187–193].

Monolithic actuators typically incorporate multiple, distinct stimuli-responsive materials or are engineered with varied microstructures to achieve multimodal operation. When exposed to a specific excitation, the responses of particular constituents or microstructural regions induce localized deformation and thereby produce actuation. Hu et al. reported a magnetoelastic millimeter-scale soft robot made from a silicone elastomer embedded with NdFeB microparticles that exhibited multimodal, magnetically controlled locomotion [15]. The robot is endowed with anisotropic magnetization before actuation, allowing for tailored responses to applied magnetic fields (Fig. 14(a)). For instance, under a rotating magnetic field, the robot crawls efficiently through narrow tunnels and along liquid surfaces. When exposed to a pulsating magnetic field, it performs on-demand jumps with tunable step length and

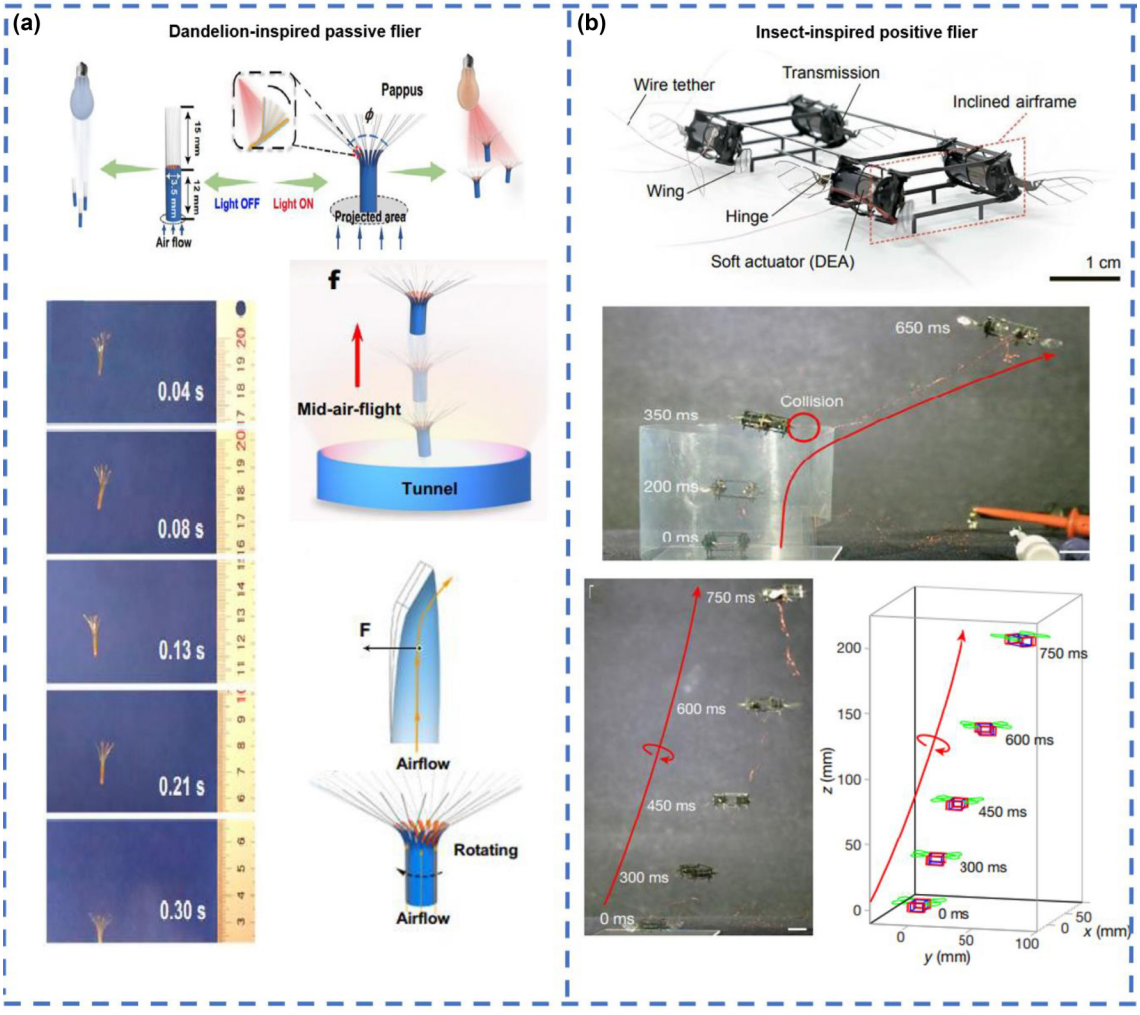

Figure 13 Flying locomotion of small-scale soft robots. (a) Dandelion-inspired passive flying locomotion. Reproduced with permission from Ref. [180], © Chen, Y. H. et al. 2023. (b) Insect-inspired active flying locomotion. Reproduced with permission from Ref. [14], © Chen, Y. F. et al. 2019.

frequency. Yang et al. designed a small-scale soft terrestrial robot equipped with DEA membranes and SMA springs, demonstrating high-performance multimodal locomotion capabilities [194]. By applying high frequency square wave signals, the DEA membrane, under voltage excitation, drove the hind limbs in a hopping gait that propelled the robot forward. By selectively activating SMA spring actuators in the forelimbs, the forelimbs underwent torsion, producing an asymmetric friction distribution at the hind ground interface and thereby affecting steering. By periodically switching the SMA springs on and off while using the DEA to control orientation, the robot executed directional jumps.

Another multi-modal locomotion method relies on the coordination of various modules of the soft robot to achieve multi-modal motion [195, 196]. Fang et al. reported an amphibian-inspired multi-modal soft robot that used three radially and symmetrically arranged soft electrohydraulic fins to achieve three locomotion modes, crawling on land and underwater, and swimming in water [197]. As shown in Fig. 14(b), periodic bending and recovery of one or two fins enabled the robot to move on the ground or in water by exploiting the friction between the fin tips and the substrate or fluid. In addition, symmetric flapping of the three fins generated upward thrust through the formation and shedding of vortex rings, thereby enabling swimming.

Multimodal locomotion integrates multiple mechanisms to enable cross-media transitions and enhanced adaptability in variable terrains. Despite its broad task coverage, this approach introduces significant integration complexity, requiring sophisticated switching strategies, stability margins, and sensor-fusion methodologies for real-time control.

4 Conclusion and perspective

This review has comprehensively examined the field of bio-inspired small-scale soft robots, with a particular emphasis on locomotion strategies enabled by functional materials. Through biological principles observed in insects, marine animals, and other organisms, researchers have developed robots capable of diverse movements like crawling, jumping, swimming, and flying. The integration of stimuli-responsive materials with bio-inspired designs has resulted in systems that demonstrate remarkable adaptability, environmental compliance, and multi-modal locomotion capabilities, showing significant potential for applications in confined space exploration, biomedical interventions, and environmental monitoring.

Looking forward, the development of bio-inspired soft robots should focus on overcoming the current limitations that hinder their practical application.

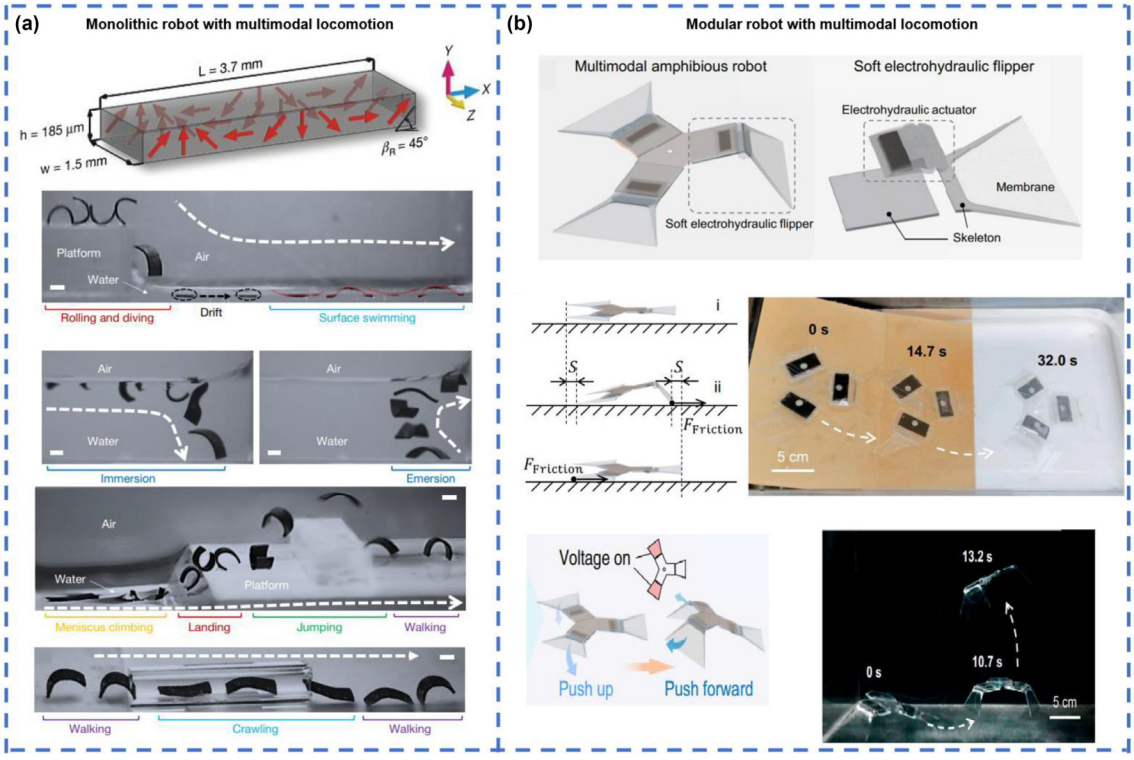

Figure 14 Multimodal locomotion of small-scale soft robots. (a) Multimodal locomotion achieved by distributing distinct stimuli-responsive materials within monolithic robot. Reproduced with permission from Ref. [193], © Macmillan Publishers Limited, part of Springer Nature 2018. (b) Multimodal locomotion achieved by coordinating modules of the soft robot. Reproduced with permission from Ref. [197], © Fang, F. Y. et al. 2025.

4.1 Bio-inspired material systems with enhanced durability

Future materials development should draw inspiration from biological systems that exhibit damage tolerance and environmental adaptation. Research directions could include creating synthetic analogs to biological composites that maintain functionality under cyclic loading, developing materials with graded properties mimicking natural tissues, and implementing biological-inspired protective mechanisms that preserve locomotion capabilities in harsh environments.

4.2 Energy systems mimicking biological efficiency

Biological organisms achieve remarkable locomotion efficiency through optimized energy storage and utilization mechanisms. Future research should explore energy harvesting systems inspired by biological metabolism, develop power management strategies similar to muscular energy allocation, and create efficient actuation systems that emulate the graded force control seen in animal movement. Particular attention should be paid to replicating the energy recovery mechanisms observed in efficient animal locomotion.

4.3 Neuromorphic control for adaptive locomotion

The development of control systems should incorporate principles from biological nervous systems to achieve the sophisticated locomotion coordination seen in nature. This includes implementing distributed control architectures inspired by central pattern generators, developing sensory-motor integration similar to biological feedback systems, and creating learning algorithms that allow robots to adapt their locomotion strategies based on environmental feedback, much like animals refine their movements through experience.

4.4 Bio-inspired manufacturing and scalability

Manufacturing approaches could incorporate biological principles of growth, scalability, and functional integration. Promising directions include developing hierarchical fabrication methods that mimic biological tissue organization, creating growth-inspired assembly processes, and implementing functional grading strategies that replicate the optimal material distribution found in natural locomotor systems.

In summary, the future development of bio-inspired soft robots will benefit from deeper integration of biological principles at all levels, from material design to locomotion control. By maintaining a strong connection to biological inspiration while addressing practical implementation challenges, the next generation of soft robots may achieve the robustness, efficiency, and adaptability required for real-world applications. The convergence of biological insight with engineering innovation will continue to drive this field toward creating robots with increasingly sophisticated and practical locomotion capabilities.

Data availability

Additional data related to this paper can be requested from the corresponding author upon request.

Acknowledgements

This work was supported by the National Natural Science Foundation of China (No. 12502219) and CNPC Innovation Found (No. 2024DQ02-0309).

Declaration of competing interest

All the contributing authors report no conflict of interests in this work.

Author contribution statement

R. T. Y.: Writing manuscript, project administration. Q. J. L.: Writing manuscript, project administration. X. L. Q.: Project administration. Y. T. L.: Project administration. Y. Y. Y.: Project administration, funding acquisition, writing manuscript. All the authors have approved the final manuscript.

Use of AI statement

None.

References

[1] Wang, B.; Shen, J.; Huang, C. Y.; Ye, Z. C.; He, J. J.; Wu, X. Y.; Guo, Z. G.; Zhang, L.; Xu, T. T. Magnetically driven biohybrid blood hydrogel fibres for personalized intracranial tumour therapy under fluoroscopic tracking. *Nat. Biomed. Eng.* **2025**, *9*, 1471–1485.

[2] Lin, Y.; Xu, Y. X.; Juang, J. Y. Single-actuator soft robot for in-pipe crawling. *Soft Robot.* **2023**, *10*, 174–186.

[3] Huang, C. Y.; Xu, T. T.; Yu, H. Y.; Wu, X. Y. A novel H-shaped soft magnetic microrobot for automatic manipulation in dynamic environments. *IEEE Trans. Autom. Sci. Eng.* **2025**, *22*, 6168–6178.

[4] Zhang, Y. X.; Wang, Q. Y.; Yi, S. Z.; Lin, Z.; Wang, C. Y.; Chen, Z. P.; Jiang, L. L. 4D printing of magnetoactive soft materials for on-demand magnetic actuation transformation. *ACS Appl. Mater. Interfaces* **2021**, *13*, 4174–4184.

[5] Li, C.; Iscen, A.; Palmer, L. C.; Schatz, G. C.; Stupp, S. I. Light-driven expansion of spiropyran hydrogels. *J. Am. Chem. Soc.* **2020**, *142*, 8447–8453.

[6] Shin, Y.; Choi, M. Y.; Choi, J.; Na, J. H.; Kim, S. Y. Design of an electro-stimulated hydrogel actuator system with fast flexible folding deformation under a low electric field. *ACS Appl. Mater. Interfaces* **2021**, *13*, 15633–15646.

[7] Ma, Y. Y.; Lu, Y.; Yue, Y. Y.; He, S. J.; Jiang, S. H.; Mei, C. T.; Xu, X. W.; Wu, Q. L.; Xiao, H. N.; Han, J. Q. Nanocellulose-mediated bilayer hydrogel actuators with thermo-responsive, shape memory and self-sensing performances. *Carbohydr. Polym.* **2024**, *335*, 122067.

[8] Weng, X.; Weng, Z. W.; Qin, M.; Zhang, J. B.; Wu, Y. C.; Jiang, H. Bioinspired moisture-driven soft actuators based on MXene/aramid nanofiber nanocomposite films. *ACS Appl. Nano Mater.* **2024**, *7*, 5587–5597.

[9] Sambyal, P.; Mahato, M.; Taseer, A. K.; Yoo, H.; Garai, M.; Nguyen, V. H.; Ali, S. S.; Oh, I. K. Magnetically and electrically responsive soft actuator derived from ferromagnetic bimetallic organic framework. *Small* **2023**, *19*, 2207140.

[10] Atia, M. G. B.; Mohammad, A.; Gameros, A.; Axinte, D.; Wright, I. Reconfigurable soft robots by building blocks. *Adv. Sci.* **2022**, *9*, 2203217.

[11] Wang, Y. B.; Du, X. Z.; Zhang, H. M.; Zou, Q.; Law, J.; Yu, J. F. Amphibious miniature soft jumping robot with on-demand in-flight maneuver. *Adv. Sci.* **2023**, *10*, 2207493.

[12] Rogóż, M.; Zeng, H.; Xuan, C.; Wiersma, D. S.; Wasylczyk, P. Light-driven soft robot mimics caterpillar locomotion in natural scale. *Adv. Opt. Mater.* **2016**, *4*, 1689–1694.

[13] Wu, S. S.; Shi, H. H.; Lu, W.; Wei, S. X.; Shang, H.; Liu, H.; Si, M. Q.; Le, X. X.; Yin, G. Q.; Theato, P. et al. Aggregation-induced emissive carbon dots gels for octopus-inspired shape/color synergistically adjustable actuators. *Angew. Chem., Int. Ed.* **2021**, *60*, 21890–21898.

[14] Chen, Y. F.; Zhao, H. C.; Mao, J.; Chirarattananon, P.; Helbling, E. F.; Hyun, N. S. P.; Clarke, D. R.; Wood, R. J. Controlled flight of a microrobot powered by soft artificial muscles. *Nature* **2019**, *575*, 324–329.

[15] Hu, W. Q.; Lum, G. Z.; Mastrangeli, M.; Sitti, M. Small-scale soft-bodied robot with multimodal locomotion. *Nature* **2018**, *554*, 81–85.

[16] Wang, Q. Z.; Xu, Z. H.; Zhao, Y. J.; Zhangsun, H.; Bu, T.; Zhang, C. Q.; Wang, X.; Wang, L. Bio-inspired self-cleaning carbon cloth based on flower-like Ag nanoparticles and leaf-like MOF: A high-performance and reusable substrate for SERS detection of azo dyes in soft drinks. *Sens. Actuators B: Chem.* **2021**, *329*, 129080.

[17] Wu, S.; Hong, Y. Y.; Zhao, Y.; Yin, J.; Zhu, Y. Caterpillar-inspired soft crawling robot with distributed programmable thermal actuation. *Sci. Adv.* **2023**, *9*, eadf8014.

[18] Zhang, L. H.; Ren, L. H.; Chen, Y. F.; Cao, Y.; Li, S. L.; Lu, W. P.; Jia, Y. Y.; Li, Y. C.; Liu, C. H.; Li, C. et al. An octopus-inspired stimulus-responsive structural color hydrogel for uterus cervical canal stent. *Adv. Healthc. Mater.* **2024**, *13*, 2400439.

[19] Chesnitskiy, A. V.; Gayduk, A. E.; Seleznev, V. A.; Prinz, V. Y. Bio-inspired micro- and nanorobotics driven by magnetic field. *Materials* **2022**, *15*, 7781.

[20] Lei, Y.; Sheng, Z. Z.; Zhang, J.; Liu, J.; Lv, W.; Hou, X. Building magnetoresponsive composite elastomers for bionic locomotion applications. *J. Bionic Eng.* **2020**, *17*, 405–420.

[21] Farhan, M.; Hartstein, D. S.; Pieper, Y.; Behl, M.; Lendlein, A.; Neffe, A. T. Bio-inspired magnetically controlled reversibly actuating multimaterial fibers. *Polymers* **2023**, *15*, 2233.

[22] Peng, Z. L.; Zhang, H.; Wang, M. J.; Zhang, S. L.; Jiang, Y. F.; Li, Y. N.; Zhu, X. Y.; Zhang, G. M.; Niu, G.; Zhang, J. et al. 3D printing bio-inspired micro soft robot with programming magnetic elastic composites. *Adv. Mater. Technol.* **2024**, *9*, 2301777.

[23] Joyee, E. B.; Pan, Y. Y. A fully three-dimensional printed inchworm-inspired soft robot with magnetic actuation. *Soft Robot.* **2019**, *6*, 333–345.

[24] Brisbois, C. A.; Tasinkevych, M.; Vázquez-Montejo, P.; de la Cruz, M. O. Actuation of magnetoelastic membranes in precessing magnetic fields. *Proc. Natl. Acad. Sci. USA* **2019**, *116*, 2500–2505.

[25] Chen, E. R.; Yang, Y. D.; Li, M. J.; Li, B. H.; Liu, G. J.; Mu, W. L.; Yin, R. Bio-mimic, fast-moving, and flippable soft piezoelectric robots. *Adv. Sci.* **2023**, *10*, 2300673.

[26] Manamanchaiyaporn, L.; Xu, T. T.; Wu, X. Y. Magnetic soft robot with the triangular head-tail morphology inspired by lateral undulation. *IEEE/ASME Trans. Mechatron.* **2020**, *25*, 2688–2699.

[27] Seong, M.; Sun, K.; Kim, S.; Kwon, H.; Lee, S. W.; Veerla, S. C.; Kang, D. K.; Kim, J.; Kondaveeti, S.; Tawfik, S. M. et al. Multifunctional magnetic muscles for soft robotics. *Nat. Commun.* **2024**, *15*, 7929.

[28] Demirörs, A. F.; Aykut, S.; Ganzeboom, S.; Meier, Y. A.; Poloni, E. Programmable droplet manipulation and wetting with soft magnetic carpets. *Proc. Natl. Acad. Sci. USA* **2021**, *118*, e2111291118.

[29] Tang, D. F.; Zhang, C. Q.; Sun, H. N.; Dai, H. Z.; Xie, J.; Fu, J. Z.; Zhao, P. Origami-inspired magnetic-driven soft actuators with programmable designs and multiple applications. *Nano Energy* **2021**, *89*, 106424.

[30] Wang, C.; Zhao, Z.; Zhang, X. S. Inverse design of magneto-active metasurfaces and robots: Theory, computation, and experimental validation. *Comput. Methods Appl. Mech. Eng.* **2023**, *413*, 116065.

[31] Huang, X.; Mutlu, H.; Theato, P. A bioinspired hierarchical underwater superoleophobic surface with reversible pH response. *Adv. Mater. Interfaces* **2020**, *7*, 2000101.

[32] Mun, S.; Lee, S.; Bae, K. J.; Bae, Y.; Lee, H. M.; Kim, B. J.; Yu, J.; Park, S. Bio-imitative synergistic color-changing and shape-morphing elastic fibers with a liquid metal core. *Adv. Fiber Mater.* **2024**, *6*, 900–910.

[33] Fan, X. J.; Sun, M. M.; Sun, L. N.; Xie, H. Ferrofluid droplets as liquid microrobots with multiple deformabilities. *Adv. Funct. Mater.* **2020**, *30*, 2000138.

[34] Gao, F.; Jiang, H. Y.; Wang, D. Y.; Wang, S. T.; Song, W. L. Bio-inspired magnetic-responsive supramolecular-covalent semi-convertible hydrogel. *Adv. Mater.* **2024**, *36*, 2401645.

[35] Cao, Y.; Li, W. J.; Quan, F. Y.; Xia, Y. Z.; Xiong, Z. Green-light-driven poly(*N*-isopropylacrylamide-acrylamide)/Fe_3O_4 nanocomposite hydrogel actuators. *Front. Mater.* **2022**, *9*, 827608.

[36] Gao, Q. F.; Pan, P. J.; Shan, G. R.; Du, M. Bioinspired stimuli-responsive hydrogel with reversible switching and fluorescence behavior served as light-controlled soft actuators. *Macromol. Mater. Eng.* **2021**, *306*, 2100379.

[37] da Cunha, M. P.; Kandail, H. S.; den Toonder, J. M. J.; Schenning, A. R. H. J. An artificial aquatic polyp that wirelessly attracts, grasps, and releases objects. *Proc. Natl. Acad. Sci. USA* **2020**, *117*, 17571–17577.

[38] Liu, M. N.; Wang, Q.; Li, A. W.; Sun, H. B. Laser defined and driven bio-inspired soft robots toward complex motion control. *Phys. Chem. Chem. Phys.* **2023**, *25*, 9753–9760.

[39] Tian, G. M.; Wen, R.; Ma, J. H.; Fu, C. Biomimetic shape-morphing actuators with controlled bending deformation and photo-mediated 3D shape programming for flexible smart devices. *Sens. Actuators B: Chem.* **2024**, *409*, 135586.

[40] Qiu, X. Y.; Guo, Q. Q.; Wang, Y. Y.; Huang, X.; Cao, J.; Zheng, Z.; Zhang, X. X. Self-healing and reconfigurable actuators based on synergistically cross-linked supramolecular elastomer. *ACS Appl. Mater. Interfaces* **2020**, *12*, 41981–41990.

[41] Bao, J. Y.; Wang, Z. Z.; Song, C. J.; Zhang, Y. H.; Li, Z. Z.; Zhang, L. Y.; Lan, R. C.; Yang, H. Shape-programmable liquid-crystalline polyurethane-based multimode actuators triggered by light-driven molecular motors. *Adv. Mater.* **2023**, *35*, 2302168.

[42] Zhang, Y. S.; Jiang, S. A.; Lin, J. D.; Lee, C. R. Bio-inspired design of active photo-mechano-chemically dual-responsive photonic film based on cholesteric liquid crystal elastomers. *J. Mater. Chem. C* **2020**, *8*, 5517–5524.

[43] Weng, M. C.; Chen, L. Z.; Huang, F.; Liu, C. H.; Zhang, W. Transparent actuator made by highly-oriented carbon nanotube film for bio-inspired optical systems. *Nanotechnology* **2020**, *31*, 065501.

[44] Yang, Y. Y.; Shen, Y. J. Light-driven carbon-based soft materials: Principle, robotization, and application. *Adv. Opt. Mater.* **2021**, *9*, 2100035.

[45] Li, K. C.; Zhang, Q.; Cui, X. Y.; Liu, Y. Y.; Liu, Y. T.; Yang, Y. Y. Photothermal-driven soft actuator capable of alternative control based on coupled-plasmonic effect. *Chem. Eng. J.* **2024**, *498*, 155057.

[46] Jia, B.; Liu, C. B.; Zhang, Y.; Tan, Y. J.; Tian, X. C.; Cui, Y. Y.; Deng, Y. Light-responsive soft robot integrating actuation and function based on laser cutting. *Micromachines* **2024**, *15*, 534.

[47] Yan, Q.; Ding, R. J.; Zheng, H. W.; Li, P. Y.; Liu, Z. L.; Chen, Z.; Xiong, J. H.; Xue, F. H.; Zhao, X.; Peng, Q. Y. et al. Bio-inspired stimuli-responsive $Ti_3C_2T_x$/PNIPAM anisotropic hydrogels for high-performance actuators. *Adv. Funct. Mater.* **2023**, *33*, 2301982.

[48] Li, C.; Iscen, A.; Sai, H.; Sato, K.; Sather, N. A.; Chin, S. M.; Alvarez, Z.; Palmer, L. C.; Schatz, G. C.; Stupp, S. I. Supramolecular-covalent hybrid polymers for light-activated mechanical actuation. *Nat. Mater.* **2020**, *19*, 900.

[49] Zheng, C. L.; Jin, F.; Zhao, Y. Y.; Zheng, M. L.; Liu, J.; Dong, X. Z.; Xiong, Z.; Xia, Y. Z.; Duan, X. M. Light-driven micron-scale 3D hydrogel actuator produced by two-photon polymerization microfabrication. *Sens. Actuators B: Chem.* **2020**, *304*, 127345.

[50] Ahmed, F.; Waqas, M.; Shaikh, B.; Khan, U.; Soomro, A. M.; Kumar, S.; Ashraf, H.; Memon, F. H.; Choi, K. H. Multi-material bio-inspired soft octopus robot for underwater synchronous swimming. *J. Bionic Eng.* **2022**, *19*, 1229–1241.

[51] Wang, M.; Jiang, C. F.; Yang, H. Electrically driven crosslinked liquid crystal polymers. *Chin. J. Chem.* **2023**, *41*, 2925–2938.

[52] Liu, Y. W.; Wu, Y. H.; Liang, H.; Xu, H. T.; Wei, Y.; Ji, Y. Rewritable electrically controllable liquid crystal actuators. *Adv. Funct. Mater.* **2023**, *33*, 2302110.

[53] Shin, J. H.; Park, J. Y.; Han, S. H.; Lee, Y. H.; Sun, J. Y.; Choi, S. S. Color-tuning mechanism of electrically stretchable photonic organogels. *Adv. Sci.* **2022**, *9*, 2202897.

[54] Wang, H. Q.; York, P.; Chen, Y. F.; Russo, S.; Ranzani, T.; Walsh, C.; Wood, R. J. Biologically inspired electrostatic artificial muscles for insect-sized robots. *Int. J. Rob. Res.* **2021**, *40*, 895–922.

[55] Chen, D. B.; Liu, Q. P.; Geng, P.; Tang, S. H.; Zhang, J. Q.; Wen, S. F.; Zhou, Y.; Yan, C. Z.; Han, Z. W.; Shi, Y. S. A 4D printing strategy and integrated design for programmable electroactive shape-color double-responsive bionic functions. *Compos. Sci. Technol.* **2021**, *208*, 108746.

[56] Ding, L.; Wu, D. H.; Wang, Q.; Wang, S.; Su, Z. L.; Zhang, D. S. Fast-response and durable liquid metal wire for wearable electronics. *Chem. Eng. J.* **2023**, *473*, 145172.

[57] Tang, W.; Lin, Y. Q.; Zhang, C.; Liang, Y. W.; Wang, J. R.; Wang, W.; Ji, C.; Zhou, M. Y.; Yang, H. Y.; Zou, J. Self-contained soft electrofluidic actuators. *Sci. Adv.* **2021**, *7*, eabf8080.

[58] Patel, D. K.; Huang, X. N.; Luo, Y. C.; Mungekar, M.; Jawed, M. K.; Yao, L. N.; Majidi, C. Highly dynamic bistable soft actuator for reconfigurable multimodal soft robots. *Adv. Mater. Technol.* **2023**, *8*, 2201259.

[59] Migliorini, L.; Santaniello, T.; Yan, Y. S.; Lenardi, C.; Milani, P. Low-voltage electrically driven homeostatic hydrogel-based actuators for underwater soft robotics. *Sens. Actuators B: Chem.* **2016**, *228*, 758–766.

[60] Zhang, X. X.; Guo, J. H.; Fu, X.; Zhang, D. G.; Zhao, Y. J. Tailoring flexible arrays for artificial cilia actuators. *Adv. Intell. Syst.* **2021**, *3*, 2000225.

[61] Haghiashtiani, G.; Habtour, E.; Park, S. H.; Gardea, F.; McAlpine, M. C. 3D printed electrically-driven soft actuators. *Extreme Mech. Lett.* **2018**, *21*, 1–8.

[62] Kotal, M.; Kim, J.; Tabassian, R.; Roy, S.; Nguyen, V. H.; Koratkar, N.; Oh, I. K. Highly bendable ionic soft actuator based on nitrogen-enriched 3D hetero-nanostructure electrode. *Adv. Funct. Mater.* **2018**, *28*, 1802464.

[63] Tu, C. M.; Chao, C. H.; Hung, S. C.; Ou, S. Y.; Zhuang, C. H.; Liu, C. Y. Bio-inspired thermal responsible liquid crystal actuators showing shape and color variations simultaneously. *J. Taiwan Inst. Chem. Eng.* **2022**, *140*, 104536.

[64] Geng, Y.; Lagerwall, J. P. F. Multiresponsive cylindrically symmetric cholesteric liquid crystal elastomer fibers templated by tubular confinement. *Adv. Sci.* **2023**, *10*, 2301414.

[65] Cui, X. C.; Liu, Z. Z.; Yi, Z. H.; Zhang, B.; Gao, X.; Fan, F. Q.; Fu, Y.; Wu, J. B.; Wang, T. Q. Reprogrammable soft actuators based on a photochromic organic-inorganic hybrid membrane with modulatable NIR photothermal conversion. *J. Colloid Interface Sci.* **2025**, *692*, 137460.

[66] Wang, W. J.; Niu, Q. Y.; Liu, X.; Su, L. N.; Zhang, J. H.; Meng, S.; Li, Z. Q.; Zhang, Y.; Xiong, Q. Q. Thermal responsive smart lanthanide luminescent hydrogel actuator. *Opt. Mater.* **2023**, *142*, 114147.

[67] Liu, Q. Y.; Wang, X. H.; Hou, Y. R.; Cheng, Y.; Zhang, J. F.; Xiao, L. Q.; Zhao, J. T.; Li, W. Bio-inspired hydrogel actuator with rapid self-strengthening behavior. *Eur. Polym. J.* **2023**, *188*, 111941.

[68] Xie, T.; Gao, Y.; Li, Z. Q.; Gao, W. A temperature-responsive dual network hydrogel for reversible smart actuator. *J. Appl. Polym. Sci.* **2024**, *141*, e55298.

[69] Lu, Y.; Ma, Y. Y.; Deng, F.; Yue, Y. Y.; Jiang, S. H.; Wu, Q. L.; Xiao, H. N.; Han, J. Q. Gradient wood-derived hydrogel actuators constructed by an isotropic-anisotropic structure strategy with rapid

thermal-response, high strength and programmable deformation. *Chem. Eng. J.* **2025**, *504*, 158903.
[70] Dai, W. T.; Zhou, X. Y.; Guo, H. L. A metal ion and thermal-responsive bilayer hydrogel actuator achieved by the asymmetric osmotic flow of water between two layers under stimuli. *Polymers* **2022**, *14*, 4019.
[71] Cui, X. C.; Liu, Z. Z.; Zhang, B.; Tang, X. D.; Fan, F. Q.; Fu, Y.; Zhang, J. H.; Wang, T. Q.; Meng, F. B. Sponge-like, semi-interpenetrating self-sensory hydrogel for smart photothermal-responsive soft actuator with biomimetic self-diagnostic intelligence. *Chem. Eng. J.* **2023**, *467*, 143515.
[72] Zou, Y.; Huang, Z. Y.; Li, X. Y.; Lv, P. Y. 4D printing pre-strained structures for fast thermal actuation. *Front. Mater.* **2021**, *8*, 661999.
[73] Hu, S. M.; Fang, Y. H.; Liang, C.; Turunen, M.; Ikkala, O.; Zhang, H. Thermally trainable dual network hydrogels. *Nat. Commun.* **2023**, *14*, 3717.
[74] Yan, J.; Xia, Y. M.; Lai, J. J.; Zhao, C. X.; Xiang, D.; Li, H.; Wu, Y. P.; Li, Z. Y.; Zhou, H. W. Stretchable and thermally responsive semi-interpenetrating nanocomposite hydrogel for wearable strain sensors and thermal switch. *Macromol. Mater. Eng.* **2022**, *307*, 2100765.
[75] Kim, T. H.; Choi, J. G.; Byun, J. Y.; Jang, Y.; Kim, S. M.; Spinks, G. M.; Kim, S. J. Biomimetic thermal-sensitive multi-transform actuator. *Sci. Rep.* **2019**, *9*, 7905.
[76] Huang, Y. C.; Cheng, Q. P.; Jeng, U. S.; Hsu, S. H. A biomimetic bilayer hydrogel actuator based on thermoresponsive gelatin methacryloyl-poly(*N*-isopropylacrylamide) hydrogel with three-dimensional printability. *ACS Appl. Mater. Interfaces* **2023**, *15*, 5798–5810.
[77] Kobayashi, K.; Yoon, C.; Oh, S. H.; Pagaduan, J. V.; Gracias, D. H. Biodegradable thermomagnetically responsive soft untethered grippers. *ACS Appl. Mater. Interfaces* **2019**, *11*, 151–159.
[78] Ji, T.; Shi, H. Y.; Yang, X. Y.; Li, H.; Kaplan, D. L.; Yeo, J.; Huang, W. W. Bioinspired genetic and chemical engineering of protein hydrogels for programable multi-responsive actuation. *Adv. Healthc. Mater.* **2024**, *13*, 2401562.
[79] Polat, D. S.; Buurman, V. E.; Mulder, D. J.; Liu, D. Q. Dual-responsive gradient structured actuator via photopolymerization-induced diffusion. *Chem.—Eur. J.* **2024**, *30*, e202400515.
[80] Houben, S. J. A.; Lugger, S. J. D.; van Raak, R. J. H.; Schenning, A. P. H. J. A pH-responsive liquid crystal hydrogel actuator with calcium-induced reprogrammable shape fixing. *ACS Appl. Polym. Mater.* **2022**, *4*, 1298–1304.
[81] Yang, C. X.; Su, F.; Xu, Y. X.; Ma, Y.; Tang, L.; Zhou, N. B.; Liang, E. X.; Wang, G. X.; Tang, J. X. pH oscillator-driven jellyfish-like hydrogel actuator with dissipative synergy between deformation and fluorescence color change. *ACS Macro Lett*. **2022**, *11*, 347–353.
[82] Pan, H. M.; Goto, A. Topology-dependent pH-responsive actuation and shape memory programming for biomimetic 4D printing. *Macromol. Rapid Commun.* **2023**, *44*, 2300074.
[83] van den Akker, W. P.; van Benthem, R. A. T. M.; Voets, I. K.; van Hest, J. C. M. Dampened transient actuation of hydrogels autonomously controlled by pH-responsive bicontinuous nanospheres. *ACS Appl. Mater. Interfaces* **2024**, *16*, 19642–19650.
[84] Sarikaya, S.; Gardea, F.; Strong, H.; Auletta, J. T.; Mackie, D. M.; Naraghi, M. Tunable actuation of humidity-driven artificial muscles via graphene nanofillers. *ACS Appl. Polym. Mater.* **2022**, *4*, 8803–8811.
[85] Jiang, S. L.; Xia, L. Bioinspired high-performance bilayer, pH-responsive hydrogel with superior adhesive property. *Polymers* **2022**, *14*, 4425.
[86] Cai, J.; Chen, Y. W.; Seyedkanani, A.; Shen, G. C.; Cerruti, M.; Akbarzadeh, A. Multifunctional and reprogrammable magnetoactive graphene oxide origami. *Adv. Sci.* **2026**, *13*, e14597.
[87] Xu, H.; Bai, S. Y.; Gu, G. Y.; Gao, Y. L.; Sun, X.; Guo, X. H.; Xuan, F. Z.; Wang, Y. M. Bioinspired self-resettable hydrogel actuators powered by a chemical fuel. *ACS Appl. Mater. Interfaces* **2022**, *14*, 43825–43832.
[88] Nan, M. M.; Guo, K. L.; Jia, T.; Wang, G. T.; Liu, S. Q. Novel acid-driven bioinspired self-resettable bilayer hydrogel actuator mimicking natural muscles. *ACS Appl. Mater. Interfaces* **2024**, *16*, 9224–9230.
[89] Kang, J. Y.; Yang, X. Y.; Yang, X. H.; Sun, J. H.; Liu, Y. H.; Wang, S. T.; Song, W. L. Carbon dots-enhanced pH-responsive lubricating hydrogel based on reversible dynamic covalent bondings. *Chinese Chem. Lett.* **2024**, *35*, 109297.
[90] Liu, Y. Q.; Chen, Z. D.; Han, D. D.; Mao, J. W.; Ma, J. N.; Zhang, Y. L.; Sun, H. B. Bioinspired soft robots based on the moisture-responsive graphene oxide. *Adv. Sci.* **2021**, *8*, 2002464.
[91] Li, H.; Li, R.; Wang, K. S.; Hu, Y. Dual-responsive soft actuator based on aligned carbon nanotube composite/graphene bimorph for bioinspired applications. *Macromol. Mater. Eng.* **2021**, *306*, 2100166.
[92] Zhao, T. T.; Liu, H.; Yuan, L.; Tian, X. M.; Xue, X. Y.; Li, T. K.; Yin, L. Q.; Zhang, J. H. A multi-responsive MXene-based actuator with integrated sensing function. *Adv. Mater. Interfaces* **2022**, *9*, 2101948.
[93] Han, Y. B.; Shi, B. R.; Xie, E.; Huang, P.; Zhou, Y. Z.; Xue, C.; Wen, W. J.; Pu, H. Y.; Zhang, M. Y.; Wu, J. B. A bio-inspired co-simulation crawling robot enabled by a carbon dot-doped dielectric elastomer. *Soft Matter* **2024**, *20*, 3436–3447.
[94] Zhang, Q. C.; Wang, M.; Ao, H. Y.; Luo, H. L.; Deng, X. Y.; Wan, Y. Z. Embedding carbon nanotube to the surfaces of poly(ε-caprolactone) film for multi-responsive actuations. *Polym. Test.* **2021**, *96*, 107086.
[95] Niu, D.; Li, D. C.; Chen, J. L.; Zhang, M. X.; Lei, B.; Jiang, W. T.; Chen, J. J.; Liu, H. Z. SMA-based soft actuators with electrically responsive and photoresponsive deformations applied in soft robots. *Sens. Actuators A: Phys.* **2022**, *341*, 113516.
[96] Cui, X. Y.; Zeng, Y. Y.; Qin, L. T.; Cheng, X.; Yang, Y. Y. Visualized sensing-integrated multi-responsive soft actuator for on-demand robotic manipulation. *Adv. Mater. Technol.* **2024**, *9*, 2302099.
[97] da Cunha, M. P.; Foelen, Y.; van Raak, R. J. H.; Murphy, J. N.; Engels, T. A. P.; Debije, M. G.; Schenning, A. P. H. J. An untethered magnetic- and light-responsive rotary gripper: Shedding light on photoresponsive liquid crystal actuators. *Adv. Opt. Mater.* **2019**, *7*, 1801643.
[98] Liu, L. K.; Li, Y. Q.; Lu, Z. C.; Miao, R. T.; Zhang, N. Thermal and light-driven soft actuators based on a conductive polypyrrole nanofibers integrated poly(*N*-isopropylacrylamide) hydrogel with intelligent response. *J. Colloid Interface Sci.* **2024**, *675*, 336–346.
[99] Zhao, T. H.; Dou, W. C.; Hu, Z. M.; Hou, W. H.; Sun, Y. R.; Lv, J. A. Reconfigurable soft actuators with multiple-stimuli responses. *Macromol. Rapid Commun.* **2020**, *41*, 2000313.
[100] Jiang, J.; Zhao, Y. Liquid crystalline elastomer for separate or collective sensing and actuation functions. *Small* **2023**, *19*, 2301932.
[101] Weng, M. C.; Ding, M.; Zhou, P. D.; Ye, Y. J.; Luo, Z. L.; Ye, X. Y.; Guo, Q. H.; Chen, L. Z. Multi-functional and integrated actuators made with bio-inspired cobweb carbon nanotube-polymer composites. *Chem. Eng. J.* **2023**, *452*, 139146.
[102] Li, Y. Q.; Xie, X.; Zhu, Q. X.; Lu, S. R.; Bai, Y. K. A novel smart composite: From self-powered sensors to multi-responsive shape memory actuators. *J. Mater. Chem. A* **2022**, *10*, 22205–22213.
[103] Belyaeva, A. A.; Eksakusto, P. O.; Morozova, S. M. Thermally and magnetically responsive single layer bioinspired soft actuator with patterned structure obtained by direct ink writing. *Mater. Today Commun.* **2024**, *39*, 108879.
[104] Wang, J. Y.; Jin, F.; Dong, X. Z.; Liu, J.; Zhou, M. X.; Li, T.; Zheng, M. L. Dual-stimuli cooperative responsive hydrogel microactuators via two-photon lithography. *Small* **2023**, *19*, 2303166.

[105] Chen, L.; Zhang, Y. L.; Zhang, K. H.; Li, F.; Duan, G. G.; Sun, Y.; Wei, X. S.; Yang, X. X.; Wang, F.; Zhang, C. M. et al. Multi-stimuli responsive, shape deformation, and synergetic biomimetic actuator. *Chem. Eng. J.* **2024**, *480*, 148205.
[106] Yin, R.; Yang, B.; Ding, X. J.; Liu, S.; Zeng, W.; Li, J.; Yang, S.; Tao, X. M. Wireless multistimulus-responsive fabric-based actuators for soft robotic, human-machine interactive, and wearable applications. *Adv. Mater. Technol.* **2020**, *5*, 2000341.
[107] Maiz-Fernández, S.; Pérez-Álvarez, L.; De Munain-Arroniz, I. L.; Zoco, A.; Lopes, A. C.; Silván, U.; Salazar, D.; Vilas-Vilela, J. L.; Lanceros-Méndez, S. Electro and magnetoactive printed bi-functional actuators based on alginate hybrid hydrogels. *Int. J. Biol. Macromol.* **2022**, *219*, 374–383.
[108] Zhang, S. N.; Wang, Z. C.; Zhang, J. Y.; Liu, J. L.; Sun, C.; Qin, S. Y.; Ren, Y. X.; Zhang, L. Y.; Hu, W.; Yang, H. Healable and multi driving mode soft actuator enabled by disulfide-bonded liquid crystal elastomers. *Chem. Eng. J.* **2024**, *491*, 152185.
[109] Huang, C. Y.; Xu, T. T.; Wu, X. Y. Leader-follower formation control of magnetically actuated millirobots for automatic navigation. *IEEE/ASME Trans. Mechatron.* **2024**, *29*, 1272–1282.
[110] Guo, Y. G.; Guo, J. L.; Liu, L. W.; Liu, Y. J.; Leng, J. S. Bioinspired multimodal soft robot driven by a single dielectric elastomer actuator and two flexible electroadhesive feet. *Extreme Mech. Lett.* **2022**, *53*, 101720.
[111] Han, L.; Si, J. W.; Guo, M. M.; Wang, R.; Wang, K.; Yang, J.; Wang, Z. Y.; Yang, X. H. An untethered soft crawling robot driven by wireless power transfer technology. *Small* **2024**, *20*, 2309661.
[112] Han, L.; Si, J. W.; Zhu, B.; Wang, R.; Wu, C. G.; Guo, M. M. A multidirectional locomotion light-driven soft crawling robot. *Adv. Funct. Mater.* **2023**, *33*, 2305046.
[113] Yang, L. L.; Chang, L. F.; Hu, Y.; Huang, M. J.; Ji, Q. X.; Lu, P.; Liu, J. Q.; Chen, W.; Wu, Y. C. An autonomous soft actuator with light-driven self-sustained wavelike oscillation for phototactic self-locomotion and power generation. *Adv. Funct. Mater.* **2020**, *30*, 1908842.
[114] Huang, C. Y.; Xu, T. T.; Li, D.; Wu, X. Y. Cooperative control strategy of multiple magnetic millirobots for automatic assembly. *IEEE/ASME Trans. Mechatron.* **2025**, *30*, 3572–3583.
[115] Çivici, U. S.; Parlar, Z. Soft robot motion under surface texture effects. *Emerg. Mater. Res.* **2020**, *9*, 226–231.
[116] Ma, W. T.; Li, B.; Jiang, L.; Wu, Y. H.; Bai, R. Y.; Chen, G. M. A soft, centimeter-scaled, thin-cable-crawling robot for narrow space inspection. *Adv. Intell. Syst.* **2024**, *6*, 2300828.
[117] Shen, D. H.; Wu, J. Y.; Wang, C. J.; Wang, X. S.; Tian, M. Q.; Adewale, O. O. Designing a soft flat crawling robot with high load capacity. *IEEE Robot. Autom. Lett.* **2021**, *6*, 5618–5625.
[118] Xu, T. T.; Huang, C. Y.; Lai, Z. Y.; Wu, X. Y. Independent control strategy of multiple magnetic flexible millirobots for position control and path following. *IEEE Trans. Rob.* **2022**, *38*, 2875–2887.
[119] Liu, Y.; Chen, B. D.; Li, W.; Zu, L. L.; Tang, W.; Wang, Z. L. Bioinspired triboelectric soft robot driven by mechanical energy. *Adv. Funct. Mater.* **2021**, *31*, 2104770.
[120] Alapan, Y.; Karacakol, A. C.; Guzelhan, S. N.; Isik, I.; Sitti, M. Reprogrammable shape morphing of magnetic soft machines. *Sci. Adv.* **2020**, *6*, eabc6414.
[121] Wang, Y. X.; Wang, J. B.; Fei, Y. Q. Design and modeling of tetrahedral soft-legged robot for multigait locomotion. *IEEE/ASME Trans. Mechatron.* **2022**, *27*, 1288–1298.
[122] Wu, Q. X.; Qiu, Z. H.; Ma, Y. Z.; Fang, Y. C.; Sun, N. Crocodile-inspired soft robots with spatial bending leg actuators and coordinated locomotion planning for amphibious environments. *IEEE Trans. Ind. Electron.* **2025**, *72*, 14553–14562.
[123] Naderinejad, M.; Junge, K.; Hughes, J. Exploration of the design of spiderweb-inspired structures for vibration-driven sensing. *Biomimetics* **2023**, *8*, 111.
[124] Li, Y. Q.; Li, Y. J.; Ren, T.; Xia, J. T.; Liu, H.; Wu, C. C.; Lin, S. Y.; Chen, Y. H. An untethered soft robotic dog standing and fast trotting with jointless and resilient soft legs. *Biomimetics* **2023**, *8*, 596.
[125] Steele, A. G.; Etoundi, A.; Hunt, A. J. Experimental verification of kinematics and kinetics in a biomimetic bipedal robot. *J. Mech. Robot.* **2023**, *15*, 014503.
[126] Smith, G. L.; Tyler, J. B.; Lazarus, N.; Tsang, H.; Viornery, L.; Shultz, J.; Bergbreiter, S. Spider-inspired, fully 3D-printed micro-hydraulics for tiny, soft robotics. *Adv. Funct. Mater.* **2023**, *33*, 2207435.
[127] Niu, L. Z.; Ding, L.; Zhang, S. J.; Yang, H. G.; Gao, H. B.; Deng, Z. Q.; Liu, G. J.; Hossain, M. SoSpider: A bio-inspired multimodal untethered soft hexapod robot for planetary lava tube exploration. *Sci. China Technol. Sci.* **2023**, *66*, 3090–3106.
[128] Wu, Q. X.; Pan, L. W.; Du, F. L.; Wu, Z. S.; Chi, X. N.; Gao, F. R.; Wang, J.; Zhilenkov, A. A. An underwater biomimetic robot that can swim, bipedal walk and grasp. *J. Bionic Eng.* **2024**, *21*, 1223–1237.
[129] Wu, Q. X.; Wu, Y.; Yang, X. C.; Zhang, B. T.; Wang, J.; Chepinskiy, S. A.; Zhilenkov, A. A. Bipedal walking of underwater soft robot based on data-driven model inspired by octopus. *Front. Robot AI* **2022**, *9*, 815435.
[130] Wu, Q. X.; Yang, X. C.; Wu, Y.; Zhou, Z. J.; Wang, J.; Zhang, B. T.; Luo, Y. B.; Chepinskiy, S. A.; Zhilenkov, A. A. A novel underwater bipedal walking soft robot bio-inspired by the coconut octopus. *Bioinspir. Biomim.* **2021**, *16*, 046007.
[131] Zhu, Y. Q.; Guo, Q.; Zhang, Y. H.; Zhu, J. R.; Zhang, P. X.; Gao, M. M.; Li, D. L.; Liu, H. A walking soft robot driven by electromagnetism inside the body. *Eng. Res. Express* **2024**, *6*, 015203.
[132] Ji, Q. L.; Fu, S.; Tan, K. G.; Thorapalli Muralidharan, S.; Lagrelius, K.; Danelia, D.; Andrikopoulos, G.; Wang, X. V.; Wang, L. H.; Feng, L. Synthesizing the optimal gait of a quadruped robot with soft actuators using deep reinforcement learning. *Robot. Comput.-Integr. Manuf.* **2022**, *78*, 102382.
[133] Mercer, C.; Hosoda, N. Analysis of structure and function of ladybird leg and subsequent design and fabrication of a simplified leg structure for robotic applications. *Biomimetics* **2024**, *9*, 184.
[134] Sun, Y. L.; Pancheri, F.; Rehekampff, C.; Lueth, T. C. TurBot: A turtle-inspired quadruped robot using topology optimized soft-rigid hybrid legs. *IEEE/ASME Trans. Mechatron.* **2024**, *29*, 3193–3202.
[135] Xu, M.; Wang, G.; Rong, C. Fiber-reinforced flexible joint actuator for soft arthropod robots. *Sens. Actuators A: Phys.* **2022**, *340*, 113522.
[136] Antonelli, M. G.; Beomonte Zobel, P.; Sarwar, M. A.; Stampone, N. Seahorse-tail-inspired soft pneumatic actuator: Development and experimental characterization. *Biomimetics* **2024**, *9*, 264.
[137] Xu, M.; Rong, C.; He, L. Design and modeling of a bio-inspired flexible joint actuator. *Actuators* **2021**, *10*, 95.
[138] Yang, X.; Chen, Y. H.; Zhang, X.; Xue, P.; Lv, P. F.; Yang, Y. Z.; Wang, L.; Feng, W. Bioinspired light-fueled water-walking soft robots based on liquid crystal network actuators with polymerizable miniaturized gold nanorods. *Nano Today* **2022**, *43*, 101419.
[139] Huang, C. Y.; Lai, Z. Y.; Wu, X. Y.; Xu, T. T. Multimodal locomotion and cargo transportation of magnetically actuated quadruped soft microrobots. *Cyborg Bionic Syst.* **2022**, *2022*, 0004.
[140] Hu, J.; Nie, Z. Z.; Wang, M.; Liu, Z. Y.; Huang, S.; Yang, H. Springtail-inspired light-driven soft jumping robots based on liquid crystal elastomers with monolithic three-leaf panel fold structure. *Angew. Chem., Int. Ed.* **2023**, *62*, e202218227.
[141] Ma, Y. Q.; Wei, Y. L.; Kong, D. Y. A biologically inspired height-adjustable jumping robot. *Appl. Sci.* **2021**, *11*, 5167.
[142] Pan, Y. T.; Fan, J. Z.; Ma, W. L.; Gao, F.; Liu, G. F.; Zhao, J. Design and motion analysis of a frog-like jumping robot based on a soft body detonation drive. *Mater. Des.* **2023**, *232*, 112127.
[143] Yu, Z. Q.; Shang, J. Y.; Shi, Q.; Xia, Y. Q.; Zhai, D. H.; Wang, H.

P.; Huang, Q.; Fukuda, T. Electrically controlled aquatic soft actuators with desynchronized actuation and light-mediated reciprocal locomotion. *ACS Appl. Mater. Interfaces* **2022**, *14*, 12936–12948.

[144] Zhou, D.; Fu, Y.; Deng, J.; Sun, J.; Liu, Y. X. A bistable jumping robot with pure soft body actuated by twisted artificial muscle. In *Proceedings of 2021 27th International Conference on Mechatronics and Machine Vision in Practice (M2VIP)*, Shanghai, China, 2021, pp 388–393.

[145] Chen, R.; Zhu, X. Y.; Yuan, Z. A.; Pu, H. Y.; Luo, J.; Sun, Y. A bioinspired single actuator-driven soft robot capable of multistrategy locomotion. *IEEE Trans. Robot.* **2024**, *40*, 2149–2165.

[146] Chen, R.; Yuan, Z. A.; Guo, J. L.; Bai, L.; Zhu, X. Y.; Liu, F. Q.; Pu, H. Y.; Xin, L. M.; Peng, Y.; Luo, J. et al. Legless soft robots capable of rapid, continuous, and steered jumping. *Nat. Commun.* **2021**, *12*, 7028.

[147] Wang, J.; Zhao, T. H.; Fan, Y. Y.; Wu, H. M.; Lv, J. A. Leveraging bioinspired structural constraints for tunable and programmable snapping dynamics in high-speed soft actuators. *Adv. Funct. Mater.* **2023**, *33*, 2209798.

[148] Zhong, T. L.; Wei, F. N.; Zhai, Z. S.; Yang, W. G. An untethered miniature soft jumping robot inspired by quadrupeds. *J. Bionic Eng.* **2023**, *20*, 1467–1480.

[149] Koh, J. S.; Yang, E.; Jung, G. P.; Jung, S. P.; Son, J. H.; Lee, S. I.; Jablonski, P. G.; Wood, R. J.; Kim, H. Y.; Cho, K. J. Jumping on water: Surface tension-dominated jumping of water striders and robotic insects. *Science* **2015**, *349*, 517–521.

[150] Liu, T. Y.; Li, D. D.; Ye, J.; Li, Q.; Sheng, L.; Liu, J. An integrated soft jumping robotic module based on liquid metals. *Adv. Eng. Mater.* **2021**, *23*, 2170050.

[151] Göttler, C.; Elflein, K.; Siegwart, R.; Sitti, M. Spider origami: Folding principle of jumping spider leg joints for bioinspired fluidic actuators. *Adv. Sci.* **2021**, *8*, 2003890.

[152] Xu, L. L.; Xue, F. H.; Zheng, H. W.; Ji, Q. X.; Qiu, C. W.; Chen, Z.; Zhao, X.; Li, P. Y.; Hu, Y.; Peng, Q. Y. et al. An insect larvae inspired MXene-based jumping actuator with controllable motion powered by light. *Nano Energy* **2022**, *103*, 107848.

[153] Gorissen, B.; Melancon, D.; Vasios, N.; Torbati, M.; Bertoldi, K. Inflatable soft jumper inspired by shell snapping. *Sci. Robot.* **2020**, *5*, eabb1967.

[154] Kim, T.; Kim, J.; Yu, S. C. Development of bioinspired multimodal underwater robot "HERO-BLUE" for walking, swimming, and crawling. *IEEE Trans. Robot.* **2024**, *40*, 1421–1438.

[155] Chi, Y. D.; Hong, Y. Y.; Zhao, Y.; Li, Y. B.; Yin, J. Snapping for high-speed and high-efficient butterfly stroke-like soft swimmer. *Sci. Adv.* **2022**, *8*, eadd3788.

[156] Nguyen, D. Q.; Ho, V. A. Anguilliform swimming performance of an eel-inspired soft robot. *Soft Robot.* **2022**, *9*, 425–439.

[157] Soomro, A. M.; Lee, J. W.; Memon, F. H.; Ahmed, F.; Hussain, K.; Choi, K. H. Bioinspired multi-material PolyJet-printed frog robot for synchronous and asynchronous swimming. *J. Bionic Eng.* **2023**, *20*, 923–933.

[158] Wang, R. Q.; Zhang, C.; Zhang, Y. W.; Yang, L. C.; Tan, W. J.; Qin, H. S.; Wang, F. F.; Liu, L. Q. Fast-swimming soft robotic fish actuated by bionic muscle. *Soft Robot.* **2024**, *11*, 845–856.

[159] Wang, Z.; Shi, D. N.; Wang, X. W.; Chen, Y. B.; Yuan, Z.; Li, Y.; Ge, Z. X.; Yang, W. G. A multifunctional light-driven swimming soft robot for various application scenarios. *Int. J. Mol. Sci.* **2022**, *23*, 9609.

[160] Yin, C.; Wei, F. N.; Fu, S. H.; Zhai, Z. S.; Ge, Z. X.; Yao, L. G.; Jiang, M. L.; Liu, M. Visible light-driven jellyfish-like miniature swimming soft robot. *ACS Appl. Mater. Interfaces* **2021**, *13*, 47147–47154.

[161] Liu, S. J.; Liu, C. B.; Liang, Y. H.; Ren, L. Q.; Ren, L. Design and control of an untethered robotic tuna based on a hydraulic soft actuator. *IEEE/ASME Trans. Mechatron.* **2025**, *30*, 623–633.

[162] Giorgio-Serchi, F.; Arienti, A.; Laschi, C. Underwater soft-bodied pulsed-jet thrusters: Actuator modeling and performance profiling. *Int. J. Robot. Res.* **2016**, *35*, 1308–1329.

[163] Chen, S. Q.; Xu, H.; Haseeb, F.; Fan, W. W.; Wei, Q. D. A pneumatic-hydraulic hybrid actuator for underwater soft robot swimming and crawling. *Sens. Actuators A: Phys.* **2023**, *356*, 114284.

[164] Wang, T. T.; Fan, X. T.; Koh, J. J.; He, C. B.; Yeow, C. H. Self-healing approach toward catalytic soft robots. *ACS Appl. Mater. Interfaces* **2022**, *14*, 40590–40598.

[165] Matharu, P. S.; Gong, P. Y.; Guntaka, K. P. R.; Almubarak, Y.; Jin, Y. Q.; Tadesse, Y. T. Jelly-Z: Swimming performance and analysis of twisted and coiled polymer (TCP) actuated jellyfish soft robot. *Sci. Rep.* **2023**, *13*, 11086.

[166] Chen, W. H.; Yang, S. G.; Zhu, C.; Cheng, Y. T.; Shi, Y. T.; Yu, C. P.; Liu, K. Scalable jet swimmer driven by pulsatile artificial muscles and soft chamber buckling. *Adv. Mater.* **2025**, *37*, 2503777.

[167] Tian, C. Y.; Mao, L. Y.; Yang, P.; Zhang, H.; Meng, X. H.; Xie, H. Carangiform-like magnetic milliswimmer with negative buoyancy for agile 3D navigation in confined fluid environments. *Adv. Funct. Mater.* **2025**, *35*, 2411017.

[168] Piazzoni, M.; Piccoli, E.; Migliorini, L.; Milana, E.; Iberite, F.; Vannozzi, L.; Ricotti, L.; Gerges, I.; Milani, P.; Marano, C. et al. Monolithic three-dimensional functionally graded hydrogels for bioinspired soft robots fabrication. *Soft Robot.* **2022**, *9*, 224–232.

[169] Shahsavan, H.; Aghakhani, A.; Zeng, H.; Guo, Y. B.; Davidson, Z. S.; Priimagi, A.; Sitti, M. Bioinspired underwater locomotion of light-driven liquid crystal gels. *Proc. Natl. Acad. Sci. USA* **2020**, *117*, 5125–5133.

[170] Yang, W. G.; Wang, X. W.; Teng, X. Y.; Qiao, Z. Z.; Yu, H. B. Programmable multi-stimulus-responsive whirligig beetle inspired soft robot with multifunctionality based on composite materials. *Colloids Surf. A: Physicochem. Eng. Asp.* **2024**, *693*, 134093.

[171] Bartlett, M. D.; Kazem, N.; Powell-Palm, M. J.; Huang, X. N.; Sun, W. H.; Malen, J. A.; Majidi, C. High thermal conductivity in soft elastomers with elongated liquid metal inclusions. *Proc. Natl. Acad. Sci. USA* **2017**, *114*, 2143–2148.

[172] Zhang, J. H.; Chen, Y. L.; Liu, Y.; Gong, Y. J. Dynamic modeling of underwater snake robot by hybrid rigid-soft actuation. *J. Mar. Sci. Eng.* **2022**, *10*, 1914.

[173] Liu, J.; Xu, T. T.; Guan, Y. M.; Yan, X. H.; Ye, C. W.; Wu, X. Y. Swimming characteristics of bioinspired helical microswimmers based on soft lotus-root fibers. *Micromachines* **2017**, *8*, 349.

[174] Soomro, A. M.; Memon, F. H.; Lee, J. W.; Ahmed, F.; Kim, K. H.; Kim, Y. S.; Choi, K. H. Fully 3D printed multi-material soft bio-inspired frog for underwater synchronous swimming. *Int. J. Mech. Sci.* **2021**, *210*, 106725.

[175] Guo, Q. H.; Yang, W. G.; Liu, H. B.; Wang, W. H.; Ge, Z. X.; Yuan, Z. An aquatic biomimetic butterfly soft robot driven by deformable photo-responsive hydrogel. *Soft Matter* **2023**, *19*, 7370–7378.

[176] Ishiguro, R.; Kawasetsu, T.; Hosoda, K. Effect of incorporating wing veins on soft wings for flapping micro air vehicles. *Front. Robot. AI* **2023**, *10*, 1243238.

[177] Lu, Z. X.; Xiong, Y.; Liu, H. J.; Yao, L. G.; Wang, Z. Y. Trajectory planning for jumping and soft landing with a new wheeled bipedal robot. *IEEE Trans. Industr. Inform.* **2024**, *20*, 13406–13415.

[178] Graule, M. A.; Chirarattananon, P.; Fuller, S. B.; Jafferis, N. T.; Ma, K. Y.; Spenko, M.; Kornbluh, R.; Wood, R. J. Perching and takeoff of a robotic insect on overhangs using switchable electrostatic adhesion. *Science* **2016**, *352*, 978–982.

[179] Yang, J. F.; Zhang, H.; Berdin, A.; Hu, W. Q.; Zeng, H. Dandelion-inspired, wind-dispersed polymer-assembly controlled by light. *Adv. Sci.* **2023**, *10*, 2206752.

[180] Chen, Y. H.; Valenzuela, C.; Zhang, X.; Yang, X.; Wang, L.; Feng, W. Light-driven dandelion-inspired microfliers. *Nat. Commun.* **2023**, *14*, 3036.

[181] Kim, S.; Hsiao, Y. H.; Lee, Y.; Zhu, W. K.; Ren, Z. J.; Niroui, F.; Chen, Y. F. Laser-assisted failure recovery for dielectric elastomer actuators in aerial robots. *Sci. Robot.* **2023**, *8*, eadf4278.
[182] Chen, P. C.; Shi, R.; Shen, N.; Zhang, Z. Q.; Liang, Y. X.; Li, T. R.; Wang, J. W.; Kong, D. J.; Gan, Y. C.; Amini, A. et al. Multistimuli-responsive insect-scale soft robotics based on anisotropic super-aligned VO_2 nanowire/carbon nanotube bimorph actuators. *Adv. Intell. Syst.* **2020**, *2*, 2000051.
[183] Sihite, E.; Kelly, P.; Ramezani, A. Computational structure design of a bio-inspired armwing mechanism. *IEEE Robot. Autom. Lett.* **2020**, *5*, 5929–5936.
[184] Xue, P.; Chen, Y. H.; Xu, Y. Y.; Valenzuela, C.; Zhang, X.; Bisoyi, H. K.; Yang, X.; Wang, L.; Xu, X. H.; Li, Q. Bioinspired MXene-based soft actuators exhibiting angle-independent structural color. *Nano-Micro Lett.* **2023**, *15*, 1.
[185] Liang, J. M.; Wu, Y. C.; Yim, J. K.; Chen, H. M.; Miao, Z. C.; Liu, H. X.; Liu, Y.; Liu, Y. X.; Wang, D. K.; Qiu, W. Y. et al. Electrostatic footpads enable agile insect-scale soft robots with trajectory control. *Sci. Robot.* **2021**, *6*, eabe7906.
[186] Chen, Y. F.; Xu, S. Y.; Ren, Z. J.; Chirarattananon, P. Collision resilient insect-scale soft-actuated aerial robots with high agility. *IEEE Trans. Robot.* **2021**, *37*, 1752–1764.
[187] Jiang, Y. K.; Chen, D. S.; Zhang, H. Y.; Giraud, F.; Paik, J. Multimodal pipe-climbing robot with origami clutches and soft modular legs. *Bioinspir. Biomim.* **2020**, *15*, 026002.
[188] Chellapurath, M.; Khandelwal, P.; Rottier, T.; Schwab, F.; Jusufi, A. Morphologically adaptive crash landing on a wall: Soft-bodied models of gliding geckos with varying material stiffnesses. *Adv. Intell. Syst.* **2022**, *4*, 2200120.
[189] Ahn, C.; Liang, X. D.; Cai, S. Q. Bioinspired design of light-powered crawling, squeezing, and jumping untethered soft robot. *Adv. Mater. Technol.* **2019**, *4*, 1900185.
[190] Zhang, L.; Zhang, Y. Q.; Li, F. B.; Yan, S.; Wang, Z. S.; Fan, L. X.; Zhang, G. Z.; Li, H. J. Water-evaporation-powered fast actuators with multimodal motion based on robust nacre-mimetic composite film. *ACS Appl. Mater. Interfaces* **2019**, *11*, 12890–12897.
[191] Mohaghar, M.; Connor, A. A.; Wu, S.; Zhao, R. R.; Webster, D. R. Effects of symmetry-breaking mechanisms on the flow field around magnetic-responsive material appendages that mimic swimming strokes. *Phys. Rev. Fluids* **2024**, *9*, 023101.
[192] Manna, R. K.; Shklyaev, O. E.; Balazs, A. C. Chemically driven multimodal locomotion of active, flexible sheets. *Langmuir* **2023**, *39*, 780–789.
[193] Dong, H. X.; Yang, H. T.; Ding, S.; Li, T.; Yu, H. Y. Bioinspired amphibious origami robot with body sensing for multimodal locomotion. *Soft Robot.* **2022**, *9*, 1198–1209.
[194] Yang, J.; Zhou, J. Y.; Xu, F.; Wang, H. S. Small-scale soft terrestrial robot with electrically driven multi-modal locomotion capability. *Soft Robot.* **2025**, *12*, 387–398.
[195] Mei, D.; Yu, X. F.; Tang, G. Q.; Kong, W. F.; Zhao, X.; Zhao, C.; Li, B.; Wang, Y. J. A soft crawling robot with multi-modal locomotion inspired by the movement mechanism of snake scales. *IEEE Robot. Autom. Lett.* **2024**, *9*, 7589–7596.
[196] Yu, Q. F.; Gravish, N. Multimodal locomotion in a soft robot through hierarchical actuation. *Soft Robot.* **2024**, *11*, 21–31.
[197] Fang, F. Y.; Zhou, J. F.; Zhang, Y. Z.; Yi, Y. R.; Huang, Z.; Feng, Y. C.; Tao, K.; Li, W. B.; Zhang, W. M. A multimodal amphibious robot driven by soft electrohydraulic flippers. *Cyborg Bionic Syst.* **2025**, *6*, 0253.